



**HAL**  
open science

## New insights on activity-related bone functional adaptations and alterations in Neolithic Liguria (northwestern Italy)

A. Varalli, Sébastien Villotte, I. Dori, V.S. Sparacello

### ► To cite this version:

A. Varalli, Sébastien Villotte, I. Dori, V.S. Sparacello. New insights on activity-related bone functional adaptations and alterations in Neolithic Liguria (northwestern Italy). *Bulletins et Mémoires de la Société d'anthropologie de Paris*, 2020, 10.3166/bmsap-2020-0072 . hal-03007251

**HAL Id: hal-03007251**

**<https://hal.science/hal-03007251>**

Submitted on 16 Nov 2020

**HAL** is a multi-disciplinary open access archive for the deposit and dissemination of scientific research documents, whether they are published or not. The documents may come from teaching and research institutions in France or abroad, or from public or private research centers.

L'archive ouverte pluridisciplinaire **HAL**, est destinée au dépôt et à la diffusion de documents scientifiques de niveau recherche, publiés ou non, émanant des établissements d'enseignement et de recherche français ou étrangers, des laboratoires publics ou privés.

1 **Article, reçu le 14/11/2019, accepté le 18/02/2020. 10 figures (Fig. 1, 6, 7, 8, 9**  
2 **and 10 une colonne et demi, Fig. 2, 3, 4 and 5 deux colonnes), 7 tableaux, 2**  
3 **annexes**

4  
5 **Title: New insights into activity-related functional bone adaptations and alterations in**  
6 **Neolithic Liguria (northwestern Italy)**

7 **Titre : Nouvelles connaissances sur les adaptations et altérations fonctionnelles osseuses**  
8 **liées à l'activité en Ligurie néolithique (nord-ouest de l'Italie)**

9 Authors: Varalli A<sup>1,2</sup>, Villotte S<sup>1</sup>, Dori I<sup>1,3,4</sup>, Sparacello VS<sup>1§</sup>.

10 <sup>1</sup> Univ. Bordeaux, CNRS, MC, PACEA, UMR 5199, 33615 Pessac, France.

11 <sup>2</sup> CaSEs Research Group, Department of Humanities, Universitat Pompeu Fabra, c/Triass Fargas  
12 25–27, Barcelona 08005, Spain.

13 <sup>3</sup> SABAP Soprintendenza Archeologia, Belle Arti e Paesaggio per le province di Verona, Rovigo  
14 e Vicenza, Piazza S. Fermo 3, 37121 Verona, Italy.

15 <sup>4</sup> Department of Biology, Laboratory of Anthropology, University of Florence, via del  
16 Proconsolo 12, 50122 Florence, Italy.

17 § Corresponding Author: Vitale Stefano Sparacello PACEA - UMR 5199 Université de  
18 Bordeaux Bâtiment B8 Allée Geoffroy Saint Hilaire CS 50023 33615 PESSAC  
19 CEDEX. [vitale.sparacello@u-bordeaux.fr](mailto:vitale.sparacello@u-bordeaux.fr); [ritosparacello@gmail.com](mailto:ritosparacello@gmail.com)

## 20 **Abstract**

21 This study offers a combined analysis of long bone mechanical properties (cross-sectional  
22 geometry, CSG), upper limb enthesopathies (ECs) and external auditory exostoses (EAE) among  
23 Neolithic people from Liguria (Italy). Previous CSG studies have suggested a high degree of  
24 mobility in mountainous terrain and sexual dimorphism in the upper limbs, with males more  
25 oriented towards uni-manual activities and females performing strenuous bimanual tasks. The  
26 aims of the study were to: 1) increase the sample size of the CSG study via the acquisition of

27 surface 3D models; 2) provide a solid chronological framework through direct dating, to allow  
28 for subsampling of individuals dated to the Impresso-Cardial Complex (ICC, c. 5800-5000 BCE)  
29 and the Square Mouthed Pottery Culture (SMP, c. 5000-4300 BCE); 3) integrate the results of  
30 CSG with information on ECs of the humeral epicondyles; 4) assess possible marine activities  
31 through analysis of EAEs. Results from the CSG analysis confirm previous studies, with no  
32 significant diachronic change. ECs in the humeral medial epicondyle parallel CSG adaptations:  
33 males tend to display more changes, especially unilaterally. Only one individual from the ICC  
34 period shows bilateral EAE, suggesting that marine activities were not prevalent. This study adds  
35 to our knowledge on activity patterns in the Neolithic in Liguria, and shows that integrating  
36 structural adaptations with information from specific enthesal alterations and exostoses can  
37 improve reconstructions of past habitual activities.

### 38 **Abstract French**

39 Nous avons analysé conjointement les propriétés mécaniques des os longs (géométrie des  
40 sections transverses, CSG), les enthésopathies des membres supérieurs (ECs) et les exostoses  
41 auditives externes (EAE) chez les sujets néolithiques de Ligurie. Des études antérieures des CSG  
42 ont suggéré une grande mobilité en terrain montagneux et un dimorphisme sexuel important pour  
43 les membres supérieurs, les hommes étant davantage orientés vers des activités uni-manuelles et  
44 les femmes effectuant préférentiellement des tâches bimanuelles pénibles. Nous avons 1)  
45 augmenté la taille de l'échantillon de l'étude des CSG par l'acquisition de modèles 3D de surface  
46 ; 2) fourni un cadre chronologique solide grâce à de nouvelles datations radiocarbones AMS  
47 directes, permettant un sous-échantillonnage d'individus datés du complexe Impresso-Cardial  
48 (ICC, c. 5800-5000 BC) et de la culture des Vases à Bouche carrée céramique à bec carré (SMP,  
49 c. 5000-4300 BC) ; 3) intégré les résultats sur les CSG avec des informations sur les ECs des  
50 épicondyles de l'humérus; 4) évalué les activités marines possibles par l'analyse des EAE. Les  
51 résultats de l'analyse des CSG confirment les études antérieures, sans changement diachronique  
52 significatif. Les résultats pour les ECs dans l'épicondyle médial sont similaires à ceux pour les  
53 CSG du membre supérieur : les hommes ont tendance à avoir plus de changements, surtout  
54 unilatéralement. Un seul individu (daté de l'ICC) présente une EAE bilatérale, ce qui suggère des  
55 activités marines peu répandues. En plus d'enrichir nos connaissances sur les schémas d'activité  
56 dans le Néolithique ligurien, cette étude montre que l'intégration des adaptations structurelles

57 avec les informations sur les ECs et les EAE peut améliorer les reconstructions des activités  
58 habituelles dans le passé.

59 **Keywords:** habitual activities, subsistence patterns, cross-sectional geometry, enthesal changes,  
60 enthesopathies, external auditory meatus exostosis

61 **Mots-clés :** Activités quotidiennes ; modes de subsistance ; géométrie des sections transverses  
62 des diaphyses ; changements enthésiques ; enthésopathies ; exostoses du conduit auditif externe.

63

## 64 **1. Introduction**

65 The evaluation of plastic, epigenetic activity-related morphological adaptations (structural bone  
66 properties) and alterations (enthesal changes) in skeletal remains from archaeological contexts  
67 provides insights into sociocultural phenomena such as subsistence changes, craft specialization,  
68 the origins and development of sexual division of labour and social inequalities [1]. Among these  
69 sociocultural phenomena, the Neolithic Transition, i.e. the adoption of a production economy  
70 based on the domestication of plants and animals, is “one of the fundamental structural processes  
71 of human history” [2,3], and dramatically changed several aspects of the human experience,  
72 particularly habitual subsistence-related physical activity. This subsistence shift has been the  
73 focus of several studies aiming to reconstruct activity patterns, which generally show a decrease  
74 in mobility among farmers when compared to earlier hunter-gatherers (reviews in [4-7]).

75 However, the Neolithisation of Europe was probably a mosaic of different processes of  
76 replacement and integration, frontiers and “leap-frog” movements, growth and collapse,  
77 coexistence and warfare (e.g. [8-13]). Therefore, the skeletal consequences of the adoption of the  
78 Neolithic lifestyle are best explored at a micro-regional level [14]. Few regions in Europe show  
79 such a concentration of prehistoric sites from the Upper Palaeolithic to the Metal Ages as  
80 western Liguria (north-western Italy): Neolithic funerary sites are especially numerous and  
81 concentrated mostly around the municipality of Finale Ligure, where hundreds of karstic caves  
82 can be found within a radius of a few kilometres. After the early arrival of the Neolithic  
83 Impresso-Cardial Complex (ICC; c. 5800-5000 cal BC; [15-17]), Liguria saw the spread of the  
84 Square Mouth Pottery (SMP; 5000-4300 cal BC; [16,18-20]), and later was the access road for  
85 the diffusion of the Chassean in northern Italy from France (4300-3700 cal BC; [18,21]). This

86 small strip of land between the mountains and the sea is therefore a pivotal region for our  
87 understanding of the cultural and biological dynamics that came into play during the spread and  
88 establishment of the Neolithic way of life in the western Mediterranean (e.g. [15,16, 22-25]).

89 Consequently, the functional adaptations of Ligurian Neolithic people have been the subject of  
90 several studies, especially via biomechanical analysis of long bones using the cross-sectional  
91 geometry method (CSG; review in [26,27]). For the lower limb, one of the main results of  
92 previous studies has been the discovery that the “sedentism” of Neolithic communities did not  
93 actually result in a low level of mobility, at least as inferred from lower limb biomechanics:  
94 Ligurian Neolithic individuals retained CSG properties that were more similar to those shown by  
95 Late Upper Palaeolithic hunters than by later agriculturalists, suggesting a high degree of  
96 mobility in a mountainous landscape [28,29,31,32,33]. These studies also showed evidence of  
97 significant sexual dimorphism in the degree of asymmetry of the upper limb, with males more  
98 asymmetrical, and females more symmetrical, than in modern industrialized groups and other  
99 agriculturalists [28,29,32,33]. This diverging pattern has been interpreted as indicative of a  
100 division of subsistence tasks between the sexes, in which the most strenuous and repetitive  
101 activities performed were mostly bi-manual for females, and mostly uni-manual for males [28].  
102 This has been tentatively associated with subsistence activities that are apparent in the  
103 archaeological record, the most prominent of which may have been cereal processing using large  
104 bi-manual querns ([33,34,35]) and woodworking and fodder harvesting with polished stone  
105 hatchets [28,33].

106 The Ligurian skeletal series was ideal to study human micro-regional adaptations, thanks to the  
107 small area from which it was unearthed. However, its chronological framework is more  
108 problematic. Most Neolithic layers had been excavated from the mid-19<sup>th</sup> century [36], in caves  
109 that, in some cases, showed evidence of human occupation from the Late Pleistocene to Roman  
110 times (e.g. [37,38]). Following the archaeological methods of the time [39], burials, and  
111 especially scattered human remains, were often excavated without keeping an accurate record of  
112 their spatial and stratigraphic positions. Probably due to the poor quality of the historic  
113 documentation, few burials were considered worthy of direct dating, and the individuals were  
114 labelled as likely/probably/possibly “Neolithic” or “Middle Neolithic” (which corresponds to the  
115 SMP culture in Liguria) depending on the material available about the associated culture. This

116 limited the number of individuals that could be included in previous bioarchaeological studies,  
117 and the lack of a more precise chrono-cultural attribution has constantly prevented  
118 anthropologists from providing more than general insights into Ligurian “Neolithic” biocultural  
119 adaptations.

120 To begin to overcome the limitations of the skeletal series and its documentation, two research  
121 projects (see Acknowledgements section) performed a comprehensive re-assessment of the  
122 Ligurian material, including individual burials, partially disturbed burials and assemblages of  
123 scattered human remains. Depending on the completeness of the material, the study collected the  
124 information available on the biological profile (sex, age, pathology, osteometric and non-metric  
125 traits, dental anthropology), as well as funerary information (e.g. [39]). In addition, the study  
126 undertook complete direct dating of the Ligurian skeletal collection attributed to the Neolithic (c.  
127 180 AMS dates), adding to the results from other recent studies [23,24,39,40]. The results of the  
128 dating campaign are reported in detail in another paper [41], but they indicate that the skeletal  
129 remains generally attributed to the Neolithic in Liguria span the period from the earliest  
130 Neolithic human occupation in the area through to the sixth and fifth millennium BCE, and in  
131 some cases belong to the Metal Ages or to historic times. For example, the double burial from  
132 Boragni, previously attributed to the Neolithic [42] and used in previous CSG research  
133 [30,33,43], actually dates to the Byzantine Period (1460±30 BP; 553-648 CE; Lyon-14599). The  
134 vast majority of the burials and skeletal remains fall chronologically within the period in which  
135 the Square Mouthed Pottery culture (SMP) has been attested in Liguria (c. 5000-4300 cal BCE;  
136 Table 1), with a small but significant presence of individuals belonging to an earlier phase (c.  
137 5800-5000 BC, [39]). Thanks to direct dating, this new study was able to include individuals  
138 (complete and partial skeletons) that are certainly Neolithic, and to create subsamples based on  
139 the various chrono-cultural phases of the Neolithic in Liguria.

140 Furthermore, the new chronological framework makes it possible to assess whether the  
141 functional adaptations and behavioural correlates inferred by previous studies still hold when  
142 using a better defined and homogenous Neolithic skeletal collection from the SMP, and whether  
143 any diachronic change can be detected during the Neolithic. For the lower limb, the hypothesis  
144 of high degrees of mobility has important implications in terms of Neolithic adaptive strategies,  
145 logistic mobility and energy expenditure [7]; for the upper limb, sexual dimorphism and the

146 hypothesized division of labour tap into issues of societal organization and identity, in addition  
147 to land use and energy expenditure to process food [33,34,35]. Confirmation is therefore needed  
148 that these results were not influenced by the inclusion in the sample of individuals from earlier  
149 pioneering Neolithic communities, or from the Metal Ages, for which technological/societal  
150 changes and a greater reliance on pastoralism have been proposed [43].

151 In addition, the project collected data on certain enthesal changes (ECs) that appear to correlate  
152 with habitual physical activity and are therefore ideal for integration with previous studies.  
153 Enthesal changes (ECs) are visible alterations on the skeleton at sites of tendon or ligament  
154 attachment, both fibrous (tendon or ligament attaching directly to the bone) and  
155 fibrocartilaginous (tendon or ligament attaching through transitional zones of a different  
156 composition) [44,45]. ECs have been associated with activity patterns in bioarchaeological  
157 studies, but their reliability as indicators of past behaviour is debated. It has been shown that a  
158 significant part of this issue is related to the methods used and the nature of the entheses under  
159 study [44,46-48]. Several factors have been mentioned by biological anthropologists to explain  
160 the occurrence of ECs at fibrocartilaginous sites, but three main causes can be identified from the  
161 medical literature (see [44] for a discussion): age (enthesopathies are more frequent in older  
162 individuals, especially after the age of 50), micro and macrotraumas, and systemic diseases  
163 (mainly DISH and spondyloarthropathies). Among the ECs that appear to correlate best with  
164 habitual activities, the one involving the medial epicondyle of the humerus could be related to  
165 strenuous uni-manual activities, especially those associated with the throwing motion [49-52]:  
166 ECs indeed appear to be frequent among prehistoric groups for which hunting involving  
167 throwing techniques has been hypothesized [51,52]. Given the divergent pattern of asymmetry  
168 by sex shown in the Neolithic Ligurian people described above, the study of ECs of the humeral  
169 epicondyle could provide further insights into the behavioural correlates of these upper limb  
170 adaptations and alterations.

171 Another bone alteration that may be relevant to draw inferences on behavioural correlates are the  
172 external auditory exostoses (EAEs), which are osseous exostoses that form in the external  
173 auditory canal as a result of an irritation of the periosteum. Several conditions can be responsible  
174 for this trait, but contact with cold water appears to be the main cause, and their prevalence and  
175 degree of expression has therefore been linked to the use of aquatic resources (for a review of the

176 medical and anthropological literature, see [53,54]). EAE can be considered as one of the most  
177 informative of activity-related skeletal morphologies: it has a very well-known etiology, the  
178 amount of available clinical data is substantial, and it is possible to compare frequencies between  
179 current and past populations, with only minor methodological problems [54]. Although  
180 archaeological and faunal evidence suggest continuous use of marine resources throughout the  
181 Neolithic, a particular emphasis on terrestrial resources and on the use of the mountainous  
182 territory has been proposed for Liguria, based on dietary [55,56], zooarchaeological [57] and  
183 biomechanical evidence (see above). A low prevalence of EAEs would therefore be expected  
184 among Ligurian Neolithic people.

185 The overall purpose of the study was therefore to 1) perform a new CSG analysis with the  
186 benefit of the new chronological framework, and test whether past behavioural inferences still  
187 hold; 2) integrate the results from ECs, verifying whether these alterations support or contrast  
188 with structural bone adaptations; 3) propose new considerations on land *vs* marine oriented  
189 subsistence activities through the analysis of EAEs.

## 190 **2. Materials and Methods**

191 A total of 57 skeletons from eight nearby Ligurian sites (Finalese and Val Pennavaire; Figure 1)  
192 was included in this study, although the sample size is smaller depending on the specific analysis  
193 and on the completeness of the remains (Table 1, see also the Excel file named Supplementary  
194 Information Tables A). Because EAEs can develop during adolescence [54], individuals from c.  
195 12 years old upwards were included in the study of this trait, while only individuals with fused  
196 long bone epiphyses were included in the CSG and ECs study. The osteometric measurements of  
197 two additional Ligurian Neolithic individuals were taken from the literature [42] to determine  
198 their sex via Discriminant Function Analysis (see below). Most individuals are directly dated to  
199 either the sixth or fifth millennium BCE; for the few individuals where dating failed or could not  
200 be done, the new chronological framework allows for a more robust chrono-cultural attribution  
201 based on contextual archaeological evidence, such as the presence of the stone cist for the Square  
202 Mouthed Pottery burials (Table 1; [41]).

203 **[Figure 1 (1.5 column) and Table 1 about here]**



204 The attribution of an individual to the “adult” age class was based on the completeness of  
205 epiphyseal fusion and dental maturation, integrated with dental wear [58]. The appearance of the  
206 pubic symphysis and auricular surface of the ilium was also considered [59-61]. Age at death of  
207 immature individuals was based, when possible, on dental maturation and eruption [62-64], and  
208 skeletal fusion [65-67], integrated when necessary with bone measurements [65,68].

209 The biological sex of the adult individuals in this study was re-assessed for all individuals via  
210 cranial and pelvic morphology, using the standards collected in Buikstra et al. [69], mandibular  
211 ramus flexure [70], and Bruzek [71] for the pelvic traits. Compared to previous studies, sex  
212 determination was changed for only one individual (Pollera 6246) , from male to female (cf.  
213 Table 1 with [32]). For 13 individuals, the fragmentary nature of the remains did not allow  
214 attribution based on pelvic and/or cranial features, and sex was assessed via Discriminant  
215 Function Analysis (DFA) using the postcranial osteometric measurements of the individuals  
216 whose sex was determined from pelvic traits (e.g. [72-75]). Forward and backward stepwise  
217 selection of variables was undertaken for each individual where the sex was uncertain, and the  
218 preferred model was chosen based on discriminant power, significance, number of individuals  
219 used for the equation and number of variables included in the model. Due to the remarkable level  
220 of sexual dimorphism displayed by the Ligurian sample, the DFA produced models with a  
221 classification rate ranging from 90-100%, and the posterior probabilities for attribution to a given  
222 sex was >87% for the 13 uncertain individuals. All the osteometric measurements and equations  
223 are given in Supplementary Information Tables A.

224 Biomechanical analysis of functional postcranial adaptations via the cross-sectional geometry  
225 method (CSG) is based on the notion that bone tissue optimizes to its mechanical environment so  
226 as to maintain physiological strains within normal limits [26,27]. Bone tissue is deposited in the  
227 shaft’s cross-section where mechanical loads require it to prevent strain in excess of the elastic  
228 limit, whereas below a certain strain threshold, the bone tissue is reabsorbed. By analyzing the  
229 cross-sections of the diaphysis, it is therefore possible to obtain variables that correlate with  
230 torsional bone rigidity (polar moment of area: J). Although the complexity of the factors  
231 influencing mechanical bone competence should always be taken into account when interpreting  
232 CSG results [26], it is generally assumed that variations in CSG properties correlate with activity  
233 levels and types, once the effect of body size is factored out to obtain a measure of “robusticity”

234 [27]. Recent experimental evidence on modern athletes has substantially confirmed this rationale  
235 [76,77,78]. Integration of quantitative data derived from CSG with ethnographic and  
236 archaeological information has therefore been widely used to draw inferences about past  
237 subsistence strategies, degrees of mobility and other habitual activities [6,7,79].

238 For this comprehensive re-assessment of the skeletal series, all of the preserved long bones were  
239 scanned in 3D, using the DAVID SLS-3 structured light scanner, to make a new assessment of  
240 structural diaphyseal properties. CSG properties for 20 individuals were added in this study (cf.  
241 Table 1 with [28,29,30,32,33,43]), and cross-sections were reconstructed (35% and 50% from the  
242 distal end for the humeri, and 50% for the femur and tibia) from the surface scans, which were  
243 positioned virtually according to the reference planes following Ruff [80]. The cross-sections  
244 were obtained using the “slice” function in Netfabb Standard 2018 for PC (copyright Autodesk  
245 2017), and the CSG properties calculated using a version of the SLICE program [81] adapted as  
246 a macro routine inserted in Scion Image release Beta 4.03. The “Solid CSG” method was used to  
247 estimate actual CSG properties from the periosteal contour via regression equations (provided in  
248 [43,82]), as justified in previous research [82-84]. All raw CSG data are given in Supplementary  
249 Information Tables A.

250 The variable used to quantify overall mechanical bone strength at a given diaphyseal level is the  
251 modulus  $Z_p$  section (torsional and (twice) average bending strength [85,86]). True section moduli  
252 are calculated by dividing the polar second moment of area  $J$  (torsional and (twice) average  
253 bending rigidity of the beam) by the distance from the centroid section for torsion to the  
254 outermost fibre of the section [86]. Until recently, software packages did not provide true section  
255 moduli, which were therefore approximated by dividing  $J$  by the average radius of the section or  
256 by raising  $J$  to the power of 0.73 [81,85,86]. In this study, we use the latter method, which makes  
257 the results comparable to a larger body of literature, including previous studies on the same  
258 skeletal series. Although  $J^{0.73}$  is proportional to rather than strictly equivalent to  $Z_p$ , given the  
259 substantial equivalency of the variables, this study will refer to  $J^{0.73}$  as  $Z_p$ , as done in previous  
260 research (e.g., [33]).

261 The mechanical loading on long bones is a function of physical activity, bone length and body  
262 mass [86]. To obtain a measure of “robusticity”, which is assumed to correlate with the effects of  
263 activity, the estimate of overall bone strength  $Z_p$  was scaled for size by dividing by mechanical

264 bone length (as defined in Ruff [80]) and body mass [86]. Body mass was estimated from the  
265 supero-inferior diameter of the femoral head following the guidelines in Trinkaus et al. [87].  
266 Certain osteometric measurements for the determination of the appropriate level of the cross-  
267 section and for standardization had to be estimated via regression equations based on the rest of  
268 the sample, as commonly done in studies of this kind (e.g. [87,88]). The regression equations for  
269 each estimated measurement are provided in Supplementary Information Tables A.

270 In order to characterize the prevalent use of one arm in activities causing strain, the degree of  
271 humeral bilateral asymmetry in J was calculated using the formula  $[(J_H - J_L)/J_L] \times 100$  (where  $J_H$   
272 and  $J_L$  are the higher and lower values of J between the two humeri, respectively) and expressed  
273 as a percentage, following previous studies [32,33,89,90]. The resulting value represents an  
274 absolute (non-directional) asymmetry. Asymmetry was calculated from the absolute values of J  
275 (i.e. not standardized by body size), because any prior size standardization would be elided.

276 Given their correspondence with mobility levels [76,78,91], lower limb CSG shape indices were  
277 also analyzed. For the femur, the ratio between  $I_x$  (second moment of area in the anteroposterior  
278 plane) and  $I_y$  (second moment of area in the mediolateral plane) was considered. For the tibia, the  
279 ratio of  $I_{max}$  (maximum second moment of area) to  $I_{min}$ , (minimum second moment of area) was  
280 used.

281 Enthesal changes (EC) in the humeral medial and lateral epicondyles were recorded. Due to the  
282 very small sample size, age-at-death is not controlled for in this study. Therefore, ECs at the  
283 lateral epicondyle were scored in order to provide a basis for comparison for the EC frequencies  
284 and distribution at the medial epicondyle. Recently, it has been found increasingly relevant to  
285 distinguish two areas for the medial epicondyle [92,93]. Thus, unlike in previous studies (i.e.  
286 [48,51,52]), the area of the medial epicondyle was divided into two zones: the area of attachment  
287 of the common flexor tendon (CFT) and the area of attachment of the anterior band of the ulnar  
288 collateral ligament (UCL). ECs at the lateral epicondyle and the area of attachment of the CFT in  
289 the medial epicondyle were scored on a 3-stage scale (A, B, C) following Villotte [46]. Several  
290 changes at the attachment of the UCL were recorded (as absent or present): erosions and  
291 cavitations of the surface, and geodes, were scored as ECG; longitudinal fissures and well-  
292 defined pits with no clear interruption of the bone surface were scored as FP (see [92]:24; Figure  
293 2). One of these features was enough to consider a change as present at the UCL attachment site.

294 A composite variable for the whole medial epicondyle (ME) was then created, merging the data  
295 for the UCL and CFT attachment sites. EC at the ME was considered as present if any change at  
296 the attachment sites of the CFT (stage B or C) and/or at the UCL was recorded. All raw data for  
297 EC are given in Supplementary Information Tables A. Asymmetry in ECs was assessed as the  
298 difference in scores between left and right sites for a given variable in a given individual.  
299 Differences between the sexes in terms of the number of asymmetrical individuals were assessed  
300 using Fisher's exact test. Differences between left and right sides within each sex in the  
301 presence/absence or aggregated score of a certain trait were also assessed using Fisher's exact  
302 test, although the independence assumption does not hold for paired humeri.

303 **[Figure 2 (2 columns) about here]**

304 EAEs were investigated through visual inspection of the auditory meatus under appropriate  
305 lighting, and recorded using a scoring system of the extent of occlusion previously applied by  
306 biological anthropologists (e.g. [94-97] and by clinicians (e.g. [98,99]). All raw data for EAEs  
307 are given in Supplementary Information Tables A.

308 The comparative samples for CSG properties consist of European Late Upper Palaeolithic (c.  
309 20,000-10,000 BCE) and Italian Iron Age (Orientalizing-Archaic Period, c. 800-500 BCE,  
310 Abruzzo region) individuals collected during previous research [31,33,79,88,100,101].

### 311 **3. Results**

#### 312 *3.1. Cross-sectional geometry*

313 Figures 3 and 4 show the main upper and lower limb CSG properties of the Ligurian sample,  
314 divided by sex and by chronological phases (c. 5800-5000 BCE: Impresso-Cardial Complex,  
315 ICC; c. 5000-4300 BCE: Square Mouthed Pottery, SMP). Note that the only individual dated to  
316 the Chassean (c. 4300-3700 BCE), for which only the left humerus could be analyzed, was not  
317 included in the figures. Raw data by individual are given in Supplementary Information.

318 Although the sample size of the ICC individuals does not allow for a clear recognition of  
319 diachronic trends, their values are within the range of variability of SMP individuals for all the  
320 variables, in both the upper (Figure 3) and lower limbs (Figure 4).

321 **[Figures 3 and 4 (both 2 columns) about here]**

322 Figure 5 and Table 2 show the comparison between upper limb CSG properties of SMP males  
323 and females when compared to Late Upper Palaeolithic hunter-gatherers and Iron Age agro-  
324 pastoralists. A diachronic trend of increasing robusticity in both humeri can be observed in  
325 males, although the SMP sample is not significantly different to LUP and IRON (Table 2).  
326 Humeral mid-distal bilateral asymmetry in SMP males is significantly lower than in LUP, but  
327 not significantly different to that in IRON males. Conversely, SMP females have the lowest  
328 asymmetry, although the comparison with IRON females is not significant at the  $\alpha = 0.05$  level  
329 after correcting for multiple comparisons (Table 2). Sexual dimorphism in the SMP sample is  
330 significant for right humeral robusticity and humeral bilateral asymmetry, with males showing  
331 higher values than females.

332 **[Figure 5 (2 columns) and Table 2 about here]**

333 Figures 6 and 7 and Table 2 show the comparison between lower limb CSG properties of SMP  
334 males and females when compared to Late Upper Palaeolithic hunter-gatherers and Iron Age  
335 agro-pastoralists (for this study the SMP individual Bergeggi 2 was not included, due to lower  
336 limb bending deformities probably due to rickets). No significant difference in femoral  
337 robusticity is present among the diachronic samples, while SMP females have higher tibial  
338 robusticity than IRON females (Figure 6, 7 and Table 2). A trend of temporally declining shape  
339 indices is observable in both the femur (Figure 6) and tibia (Figure 7), the decrease being  
340 particularly marked between SMP and IRON individuals especially. Both sexes in the SMP  
341 sample have significantly higher femoral shape indices than their IRON counterparts after  
342 correcting for multiple comparisons (Table 2). Sexual dimorphism in the SMP sample is  
343 significant for the shape indices of both the femur and tibia, the males showing higher values  
344 than females (Table 2).

345 **[Figures 6 and 7 (both 1.5 column) about here]**

### 346 *3.2 Humeral enthesal changes*

347 Table 3 shows the results of the evaluation of enthesal changes in the medial and lateral  
348 epicondyle of the humerus. For the lateral epicondyle, in both sides and in both sexes, ECs are  
349 frequent (ca. 50% of the lateral epicondyles present stage B or C). No significant difference in  
350 the pattern of stage frequency could be detected, whether comparing sides within or between

351 sexes. When considering individuals that could be examined bilaterally, the stage of ECs in the  
352 lateral epicondyle generally shows symmetry between sides (Table 3).

353 [Table 3 about here]

354 Results for the medial epicondyle differ from the lateral epicondyle in many ways. When  
355 considering the area of attachment of the CFT, no individual in the SMP or larger Ligurian  
356 Neolithic sample shows stage C. Stage B appears to be more represented in the right CFT area in  
357 males, but no variation by side or by sex is statistically significant. However, when considering  
358 individuals that could be examined bilaterally, males have consistently higher scores in the right  
359 CFT area when compared to females, which are more symmetrical. This result is significant at  
360 the  $\alpha = 0.05$  level after pooling the SMP and ICC individuals (Table 4).

361 [Table 4 about here]

362 Changes at the UCL attachment site are present in both sexes, but especially on the right side in  
363 males. Males have more lesions than females on the right side, but not on the left. Asymmetrical  
364 individuals are significantly more frequent in males than in females (Table 5)

365 [Table 5 about here]

366 When the CFT and UCL scores are aggregated, obtaining the “any change” variable for the  
367 medial epicondyle (ME any change), the pattern is similar to that described above: males show  
368 more changes especially on the right side, and asymmetrical individuals are more frequent in  
369 males than in females (Tables 6 and 7). However, the results are no longer statistically  
370 significant, probably due to the smaller sample size, when considering only individuals for which  
371 both the CFT attachment site and the anterior band of the UCL could be scored (Table 6). When  
372 aggregating the scores for individuals to which at least one score could be attributed, the results  
373 are statistically significant in the SMP sample (Table 7).

374 [Tables 6 and 7 about here]

375 No significant difference in humeral robusticity (both mid-distal and midshaft  $Z_p$ ) or humeral  
376 bilateral asymmetry (mid-distal and midshaft HUMBA), as described by CSG data, could be  
377 detected between the subsamples based on sex and the medial/lateral epicondyle stage of  
378 enthesal change (Supplementary Information Tables B). However, SMP individuals (pooled

379 sexes) with asymmetrical CFT stages of enthesal change tend to have more robust right and left  
380 humeri as described by mid-distal  $Z_p$  (T-test  $p < 0.05$ ; Supplementary Information Table B-2).  
381 Furthermore, in both in the pooled Ligurian Neolithic sample and the SMP sample, individuals  
382 with changes at the UCL (pooled sexes) show more robust right and left humeri as described by  
383 mid-distal  $Z_p$  (T-test  $p < 0.05$ ), and more asymmetrical humeri as described by the mid-distal  
384 bilateral asymmetry in  $Z_p$  (T-test  $p < 0.05$ ; Supplementary Information Tables B-3 and B-4).  
385 Although the significance of these results is mostly due to the observed sexual dimorphism in  
386 robusticity and asymmetry (Table 2) and in the higher prevalence of changes in the UCL in  
387 males (Table 5), it may be noticed that the same pattern is present by sex, although the results are  
388 not statistically significant (Figure 8).

389 Furthermore, a correspondence between changes in the UCL (ECG or ECG+FP) and humeral  
390 robusticity, asymmetry and laterality can be inferred from the categorized scatterplots (Figure 9).  
391 More robust and asymmetrical individuals will tend to have changes in the UCL, and the only  
392 individual with ECG on the left humerus is also the most asymmetrical left-dominant individual  
393 (Figure 9a). When considering the aggregate score for the medial epicondyle (ME any change)  
394 the correspondence between enthesal changes and CSG robusticity and laterality is less  
395 apparent, when considering only individuals for which both CFT and UCL could be scored  
396 (Figure 9c, and see above), and when including individuals to which only one score could be  
397 attributed (Figure 9d).

398 **[Figures 8 and 9 (both 1.5 column) about here]**

### 399 *3.3 external auditory canal exostosis (EAE)*

400 Among the 30 individuals that could be observed for EAE (Supplementary Information Table  
401 A), only one male individual dating to the sixth millennium BCE (Arma dell'Aquila 1 Richard)  
402 displays slight bilateral EAEs (Figure 10).

403 **[Figure 10 (1.5 column) about here]**

## 404 **4. Discussion**

405 This study aimed to reassess functional adaptations in the Ligurian Neolithic skeletal series,  
406 based on the new chronological framework recently provided by direct dating [39,41]. In

407 addition to verifying whether the inferences on subsistence-related activity patterns made in the  
408 past using CSG (e.g. [28,30]) still hold, this study added new observations on certain enthesal  
409 changes that appear to correlate with habitual physical activity, located in the distal humerus  
410 [46,92] and in the external auditory meatus [54,97].

411 The direct dating results confirm that most of the skeletal series from Liguria overlap  
412 chronologically with the Square Mouthed Pottery culture (SMP), c. 5000-4300 BCE, i.e. the  
413 “Middle Neolithic” of Liguria [41]. With the new chronological framework, it became possible  
414 to attribute several individuals to this period, for which direct dating had failed or which could  
415 not be sampled, based on funerary treatment (e.g. Arene Candide 6PE, Arene Candide II BB,  
416 Pollera 32PE; [41]). On the other hand, certain individuals included in previous studies could no  
417 longer be assigned to the Neolithic (e.g. Boragni), or were assigned to a cultural tradition earlier  
418 than the SMP within the Impresso-Cardial Complex (ICC; e.g. most of the individuals from  
419 Arma dell’ Aquila; [39]). Despite the exclusion of these individuals from the SMP sample, the  
420 Ligurian “Middle Neolithic” sample size for CSG analysis is still slightly larger than in previous  
421 studies, thanks to the inclusion of CSG data from 20 additional individuals that were excluded  
422 from previous analyses due to the lack of chrono-cultural attribution.

423 The characterization of functional adaptations of Ligurian SMP people does not change  
424 significantly based on this revised sample, which confirms the validity of previous observations  
425 and inferences on subsistence patterns [28-30,32,33]. The small size of the ICC sample does not  
426 allow for inferences on diachronic trends; however, most ICC individuals do not seem to deviate  
427 from the variability of the SMP sample. Lower limb CSG properties are still compatible with  
428 high levels of mobility in rugged terrain [30,31], showing values that are closer to Late  
429 Palaeolithic hunter-gatherers than later protohistorical agro-pastoralists. This further highlights  
430 how subsistence activities, particularly logistic mobility, among early agro-pastoralists in this  
431 region may have differed from later, more specialized forms of pastoralism [33]. However, more  
432 studies on controlled athlete *vs* sedentary samples are necessary to fully understand how different  
433 types of mobility influence femoral and tibial robusticity and lead to specific cross-sectional  
434 shapes (cf. our results with [76,78]).

435 The degree of asymmetry in humeral mid-distal mechanical rigidity of SMP males, around 20%,  
436 is lower than that shown by LUP hunters, whose subsistence activities probably included a



437 substantial amount of throwing [88], and later Iron Age agro-pastoralists, who performed uni-  
438 manual sword training [33,79,100]. However, SMP male asymmetry is still relevant when  
439 compared to “physiological” asymmetry (8-12%; [77,89]), and especially when compared to  
440 SMP females, which show the lowest asymmetry among the comparative groups. The three  
441 females in the ICC sample show very low levels of mid-distal humeral asymmetry (between 2-  
442 4%), suggesting that this trait was shared among Neolithic females in Liguria (less relevant for  
443 behavioural inferences is their relatively higher asymmetry at midshaft of the humerus, which is  
444 often influenced by the shape of the deltoid tuberosity [79]). Previous studies have suggested a  
445 possible causal relationship between the diverging pattern of asymmetry in males and females  
446 and the division of labour (see Introduction). However, caution is needed when inferring division  
447 of labour based on sexual dimorphism in structural properties, given the possible influence of  
448 hormonal factors and body size (34,88). In this research, the focus was on determining whether  
449 CSG and ECs in the humerus produced compatible results.

450 Both CSG and ECs have been widely used in the past to draw inferences about activity patterns,  
451 although many studies have warned against simplistic interpretations of results given the number  
452 of concomitant factors that influence mechanical bone competence, enthesal appearance and  
453 other “markers of activities” (e.g. [26,102,103]). In particular, age and body size appear to be  
454 confounding factors for both methods. For CSG, mechanical properties seem to mostly reflect  
455 levels of activity during the pre- and peri-pubertal periods, while the extent of remodelling due to  
456 activity in later life is debated [26,27,104]. In addition, senescence does influence CSG  
457 properties, due to continued periosteal apposition to mechanically compensate for medullary  
458 expansion (especially in males; [105,106]). These limitations are presumed to have a relatively  
459 minor impact on the inferences about habitual activity and subsistence drawn from  
460 bioarchaeological samples, since it is assumed that individuals in prehistoric societies  
461 participated in subsistence activities as from late childhood, and died before reaching senescence.  
462 Hormonal and genetic factors may nevertheless confound behavioural interpretations [34,107].  
463 In contrast, for ECs, the whole correlation with activity patterns is brought into question once  
464 age and body size are taken into account (e.g. [108-110]). Studies integrating CSG and ECs  
465 results for bioarchaeological reconstructions of activity patterns have at best found a general  
466 correspondence between the two methods (e.g. [111]), and more detailed tests between ECs  
467 scores and CSG values have failed to provide a consistent association [110,112-114]. This study

468 has found similar results: individuals with higher scores in medial and lateral humeral epicondyle  
469 ECs are not consistently more robust. However, rather than expecting a general correspondence  
470 between EC scores and CSG robusticity, it is possible that specific enthesal changes, and  
471 especially their asymmetry, may be indicative of certain habitual activities.

472 The shape of the humeral medial epicondyle appears to have an influence on the pronation-  
473 supination range during elbow flexion and extension [115], and ECs in this area have been  
474 associated with trauma resulting from powerful extensions of the forearm, possibly related to  
475 throwing [49,50-52]. Prehistoric groups, especially Upper Palaeolithic hunters, often appear to  
476 show lesions in this area [51,52]. Among Upper Palaeolithic hunters, throwing has also been  
477 considered to be one of the main factors determining the remarkable degree of asymmetry in  
478 humeral mechanical rigidity, which is comparable or greater than that shown in professional  
479 tennis players or, indeed, throwers (e.g. [88]). A relationship between ECs in the medial  
480 epicondyle and CSG properties, particularly asymmetry, was therefore expected. Accordingly, in  
481 this study there is agreement between the inferences that could be drawn based on CSG and  
482 medial epicondyle ECs: males tend to be more asymmetrical than females, and tend to have  
483 lesions on the right side more frequently. In addition, although the sample size is small, there  
484 appears to be, within sexes, a correspondence between the presence of lesions in the dominant  
485 arm, in the anterior band of the UCL, and the level of humeral asymmetry. This relationship  
486 seems to be consistent with the laterality of CSG asymmetry: the only individual with somewhat  
487 relevant left-sided asymmetry is also the only individual with an erosion in the left anterior band  
488 of the UCL. However, this possible correspondence between biomechanical properties and ECs  
489 becomes less discernible when aggregating other enthesal changes in the medial epicondyle,  
490 further suggesting that, among ECs, erosions in the UCL may be particularly relevant for  
491 reconstructing activity. The very small sample size, however, makes these considerations  
492 speculative. Further research using a large sample with known activity is necessary to confirm  
493 the results found here.

494 In the Neolithic Ligurian sample, only one case of bilateral EAE (grade 1) has been recorded, in  
495 an individual from the ICC, Arma dell'Aquila 1. It is difficult to discuss frequencies of EAEs in  
496 a small sample [54]: although the total sample of Neolithic crania is 30, only three other  
497 individuals from the ICC period could be examined for EAE, and only unilaterally

498 (Supplementary Information Table A). More archaeological and biochemical data on Neolithic  
499 Ligurian people are needed to understand whether this result could be compatible with a greater  
500 focus on marine resource use in the ICC Neolithic. No significant consumption of fish protein  
501 during the ICC and SMP periods has been proposed in light of the collagen isotopic composition  
502 of human bone [40,55,56]. However, archaeological and faunal evidence (e.g. shells, fish bones,  
503 fishing hooks, shell blow horns) are evidence of the continuous use of marine resources  
504 throughout the Neolithic [116]. In addition, EAE may be due to causes other than frequent  
505 contact with cold water, including infection, eczema, trauma and other pathological conditions  
506 affecting the normal homeostasis of the external ear canal [117,118]. Finally, the absence of  
507 EAE does not exclude aquatic activities. However, it should be noted that in populations for  
508 which isotopic data has indicated significant reliance on aquatic resources, EAEs tend to be very  
509 frequent and the occlusion of the ear canal is sometimes severe (i.e.; grades 2 or 3)  
510 [54,94,97,119], which is not the case here. The results, although caution is necessary given the  
511 small sample size, seem compatible with a subsistence scenario where marine resource use was  
512 of relatively minor importance.

## 513 **5. Conclusions**

514 This study performed a re-assessment of long bone structural properties in the Neolithic Ligurian  
515 skeletal series, in the light of the new chronological framework produced by direct dating and  
516 new data derived by 3D scanning of the entire assemblage of long bones. As well as considering  
517 the plastic adaptation of the diaphyses, this study included an interpretative scenario with new  
518 data from skeletal alterations that are considered to be correlated with habitual activities. The  
519 analysis included enthesal changes in the humeral epicondyles, which have been associated  
520 with vigorous exertion of the upper limb, including the throwing motion, and the presence of  
521 exostoses in the external auditory meatus, which are considered to be an indicator of aquatic  
522 activities.

523 The biomechanical analysis results confirm previous studies: the data for lower limbs suggest  
524 high mobility; the upper limb is robust in both sexes, but males show significantly higher  
525 humeral asymmetry than females. No diachronic change was apparent when considering the  
526 subsampling based on chrono-cultural complexes within the Neolithic. Enthesal alterations in  
527 the humeral medial epicondyle are consistent with the results obtained from structural

528 adaptations: males tend to show more changes than females, especially unilaterally on the more  
529 mechanically robust side. In addition, individuals with lesions in the medial epicondyle tend to  
530 have higher asymmetry. This result is potentially important because studies on adaptations and  
531 alterations have often failed to produce consistent results. However, the sample size is very  
532 small, and more research is necessary to confirm this correspondence between results derived  
533 from structural adaptations and bone alterations.

534 Only one individual from the sixth millennium BCE shows bilateral external auditory meatus  
535 exostosis, supporting the archaeological evidence suggesting that marine activities were not  
536 prevalent during the Neolithic in Liguria. However, again, the sample size is too small, and  
537 further evidence is necessary to investigate this issue.

538 This study has added to our knowledge on activity patterns in the Neolithic in Liguria, and  
539 supports the careful integration of data on structural adaptations with information from specific  
540 enthesal alterations and exostoses to draw inferences about past habitual activities.

541

## 542 **Acknowledgements**

543 The authors would like to thank the Soprintendenza Archeologia, Belle Arti e Paesaggio per la  
544 città metropolitana di Genova e le provincie di Imperia, La Spezia e Savona, for granting access  
545 to skeletal collections, Superintendent Vincenzo Tiné and Officers Elisabetta Starnini, Marta  
546 Conventi, Nico Radi, and Stefano Costa. We are grateful to the directors, curators, and staff of  
547 the museums where the skeletal collections are preserved for their continuous assistance during  
548 data collection: Daniele Arobba and Andrea De Pascale (Museo Archeologico del Finale, Finale  
549 Ligure), Patrizia Garibaldi, Guido Rossi, Irene Molinari (Museo di Archeologia Ligure, Genova),  
550 and Monica Zavattaro (Museo di Storia Naturale – Sezione di Antropologia e Etnologia,  
551 Università degli Studi di Firenze). Thanks to Camillo Costa and the staff of the Museo Navale  
552 Romano di Albenga. Thanks to Chiara Panelli, Stefano Rossi, Roberto Maggi, Vincenzo  
553 Formicola, Paolo Biagi, Giovanni Murialdo, Gwenaëlle Goude, Sara Bernardini, Claudia Ferro,  
554 Giuseppe “Cisque” Vicino, Maria Tagliafico, Elisa Bianchi, Simona Mordeglia, Walter  
555 Siciliano, Jacopo Moggi-Cecchi, Giovanna Stefania, Luca Bachechi, Chiara Bullo and Brunetto  
556 Chiarelli for their assistance during data collection and their scientific input.

557 For their continuous assistance during the analysis, we are grateful to all the staff of the  
558 University of Groningen Centre for Isotope Research (CIO), to Christine Oberlin, Centre de  
559 Datation par le RadioCarbone, Université Claude Bernard Lyon1, and to Lucile Beck,  
560 Responsable de la Plateforme Nationale LMC14 Laboratoire de Mesure du Carbone 14  
561 (CEA/CNRS/IRD/IRSN/MCC)-LSCE CEA Saclay. The AMS dating performed at the Centre de  
562 Datation par le RadioCarbone was supported by the “ARTEMIS” program.

563 The BUR.P.P.H project: Burial practices at the Pleistocene - Holocene transition: the changing  
564 role of pathology, violence, and “exceptional events” (PI: VSS) received financial support from  
565 the French State under the “Investing for the Future” Program, IdEx Bordeaux, reference ANR-  
566 10-IDEX-03-02. The DEN.P.H. project: Dental anthropology at the Pleistocene-Holocene  
567 transition – insights on lifestyle and funerary behaviour from Neolithic Liguria (Italy) (PI: ID) is  
568 funded by the European Union’s Horizon 2020 research and innovation program under the Marie  
569 Skłodowska-Curie grant agreement No 752626.

570

## 571 **Literature Cited**

- 572 1. Knüsel CJ, Sparacello V (2018) Functional morphology, postcranial, human. In:Trevathan  
573 W, Cartmill M, Dufour D, Larsen C, O’Rourke D, Rosenberg K, Strier K (eds) The  
574 International Encyclopedia of Biological  
575 Anthropologydoi:10.1002/9781118584538.ieba0187
- 576 2. Bocquet-Appel J-P (2011a) When the world’s population took off: the springboard of the  
577 Neolithic Demographic Transition. *Science* 333:560–561
- 578 3. Bocquet-Appel J-P (2011b) The agricultural demographic transition during and after the  
579 agriculture inventions. *Curr Anthropol* 52:S497–S510
- 580 4. Larsen CS (1995) Biological changes in human populations with agriculture. *Ann Rev*  
581 *Anthropol* 24:185–213
- 582 5. Larsen CS (1997) *Bioarchaeology*, Cambridge University Press, Cambridge, 461 p
- 583 6. Pinhasi R, Stock J (eds) (2011) *Human bioarchaeology of the Transition to*  
584 *Agriculture*, Wiley-Liss, New York, 488 p
- 585 7. Carlson K, Marchi D (eds) (2014) *Reconstructing mobility: environmental, behavioral, and*  
586 *morphological determinants*, Springer, New York, 295 p

- 587 8. Lahr M, Foley R, Pinhasi R (2000) Expected regional patterns of Mesolithic-Neolithic  
588 human population admixture in Europe based on archaeological evidence. In: Renfrew C,  
589 Boyle K (eds) *Archaeogenetics: DNA and the Population Prehistory of Europe*. McDonald  
590 Institute for Archaeological Research, Monographs, Cambridge, pp 81–88
- 591 9. Clare K, Rohling EJ, Weninger B, et al (2008) Warfare in Late Neolithic/Early Chalcolithic  
592 Pisidia, southwestern Turkey. Climate induced social unrest in the late 7th millennium cal  
593 BC. *Doc Praehist* 25:65–92
- 594 10. Zeder MA (2008) Domestication and early agriculture in the Mediterranean basin: origins,  
595 diffusion, and impact. *PNAS* 105(33):11597–11604
- 596 11. Rowley-Conwy P (2011) Westward Ho! The spread of agriculture from Central Europe to  
597 the Atlantic. *Curr Anthropol* S52:431–451
- 598 12. Shennan S, Downey SS, Timpson A, et al (2013) Regional population collapse followed  
599 initial agriculture booms in mid-Holocene Europe. *Nat Comm* 4:2486
- 600 13. Meyer C, Lohr C, Gronenborn D, et al (2015) The massacre mass grave of Schöneck-  
601 Kikianstädten reveals new insights into collective violence in Early Neolithic Central Europe.  
602 *PNAS* 112(36):11217–11222
- 603 14. Stock JT, Pinhasi R (2011) Introduction. Changing paradigms in our understanding of the  
604 transition to agriculture: human bioarchaeology, behaviour and adaptation. In: Pinhasi R,  
605 Stock J (eds) *Human bioarchaeology of the Transition to Agriculture*. Wiley-Liss, New York,  
606 pp 1–17
- 607 15. Binder D (2013) *Mésolithique et Néolithique ancien en Méditerranée nord-occidentale entre*  
608 *7000 et 5500 cal. BCE: questions ouvertes sur les dynamiques culturelles et les procès*  
609 *d’interaction. Actes du XXVIIe Congrès préhistorique de France (Bordeaux–Les Eyzies,*  
610 *2010). Société préhistorique française, Paris, pp 341–355*
- 611 16. Binder D, Sénépart I (2010) La séquence de l’Impresso-Cardial de l’abri Pendimoun et  
612 l’évolution des assemblages céramiques en Provence. *Mémoire LI de la Société Préhistorique*  
613 *française, pp 149–167*
- 614 17. Binder D, Lanos P, Angeli L, et al (2017) Modelling the earliest north-western dispersal of  
615 Mediterranean Impressed Wares: new dates and Bayesian chronological model. *Doc Praehist*  
616 44:54–77

- 617 18. Maggi R (1997) The Radiocarbon Chronology. In: Maggi R (ed) *Arene Candide: a functional*  
618 *and environmental assessment of the Holocene sequence (excavations Bernabò Brea-Cardini*  
619 *1940–1950)*. Istituto Italiano di paleontologia umana, Il calamo, Roma, ns 5, pp 31–52
- 620 19. Pearce M (2013) Radiocarbon chronology for the spread of the early Neolithic north through  
621 the Tyrrhenian and Ligurian Seas area. In: Pearce M (ed) *Rethinking the North Italian Early*  
622 *Neolithic*. Accordia Research Institute, University of London, London, pp 21–84
- 623 20. Del Lucchese A, Starnini E (2015) Aggiornamenti sulla fase antica della Cultura dei Vasi a  
624 Bocca Quadrata in Liguria da una revisione dei materiali ceramici in corso. In: Conventi M,  
625 Del Lucchese A, Gardini A (eds) *Archeologia in Liguria, ns5 (2012-2013)*. Sagep Editrice  
626 Genova, pp 27–37
- 627 21. Crepaldi F (2001) Le Chasséen en Ligurie. *Bull Soc Prehistor Fr* 98(3):485–494
- 628 22. Branch NP, Black S, Maggi R, et al (2014) The neolithisation of Liguria (NW Italy): an  
629 environmental archaeological and palaeoenvironmental perspective. *Environ Archaeol*  
630 19:196–213
- 631 23. Biagi P, Starnini E (2016) La cultura della Ceramica Impressa nella Liguria di Ponente (Italia  
632 Settentrionale): distribuzione, cronologia e aspetti culturali. In: Bonet Rosado H (ed) *Del*  
633 *neolític a l’edat del bronze en el Mediterrani occidental. Estudis en homenatge a Bernat*  
634 *Martí Oliver*. TV SIP 119, València, pp 35–49
- 635 24. Biagi P, Starnini E (2018) Gli scavi all’Arma dell’Aquila (Finale Ligure, Savona): le ricerche  
636 e i materiali degli scavi del Novecento. *Quaderno 15*. Società per la Preistoria e Protostoria  
637 della Regione Friuli-Venezia Giulia, Trieste, 260 p
- 638 25. Arobba D, Panelli C, Caramiello R, Gabriele M, Maggi R (2017) Cereal remains, plant  
639 impressions and 14C direct dating from the Neolithic pottery of Arene Candide Cave (Finale  
640 Ligure, NW Italy). *J Archeol Sci: Rep* 12:395–404
- 641 26. Pearson OM, Lieberman DE (2004) The aging of Wolff’s ‘Law’: ontogeny and response to  
642 mechanical loading in cortical bone. *Am J Phys Anthropol* 47:63–99
- 643 27. Ruff CB, Holt B, Trinkaus E (2006) Who’s afraid of the big bad Wolff? ‘Wolff’s law’ and  
644 bone functional adaptation. *Am J Phys Anthropol* 129:484–498
- 645 28. Marchi D, Sparacello VS, Holt BM, et al (2006) Biomechanical approach to the  
646 reconstruction of activity patterns in Neolithic Western Liguria, Italy. *Am J Phys Anthropol*  
647 131:447–455

- 648 29. Marchi D (2008) Relationships between lower limb cross-sectional geometry and mobility:  
649 the case of a Neolithic sample from Italy. *Am J Phys Anthropol* 137:188–200
- 650 30. Sparacello VS, Marchi D, Shaw CN (2014) The importance of considering fibular robusticity  
651 when inferring the mobility patterns of past populations. In: Carlson K, Marchi D (eds)  
652 *Reconstructing mobility: environmental, behavioral, and morphological determinants*.  
653 Springer, New York, pp 91–111
- 654 31. Sparacello VS, Villotte S, Shaw CN, et al (2018) Changing mobility patterns at the  
655 Pleistocene-Holocene transition: the biomechanics of the lower limb of Italian Gravettian and  
656 Mesolithic individuals. In: Cristiani E, Borgia V (eds) *Palaeolithic Italy: Advanced studies on*  
657 *early human adaptations in the Apennine Peninsula*. Sidestone Press, Leiden, pp 357–396
- 658 32. Sparacello VS, Roberts CA, Canci A, et al (2016) Insights on the paleoepidemiology of  
659 ancient tuberculosis from the structural analysis of postcranial remains from the Ligurian  
660 Neolithic (northwestern Italy). *Int J Paleopath* 15:50-64.
- 661 33. Sparacello VS, Pearson OM, Coppa A, et al (2011) Changes in robusticity in an Iron Age  
662 agropastoral group: the Samnites from the Alfedena necropolis (Abruzzo, Central Italy). *Am*  
663 *J Phys Anthropol* 144:119–130
- 664 34. Macintosh AA, Pinhasi R, Stock JT (2014) Divergence in male and female manipulative  
665 behaviors with the intensification of metallurgy in Central Europe. *PLoS ONE*  
666 9(11):e112116
- 667 35. Sládek V, Ruff CB, Berner M, et al (2016) The impact of subsistence changes on humeral  
668 bilateral asymmetry in Terminal Pleistocene and Holocene Europe. *J Hum Evol* 92:37–49
- 669 36. De Pascale A (2008) Le prime esplorazioni nelle caverne ossifere del Finalese: tracce, ipotesi  
670 e scoperte ad opera di Issel, Perrando, Morelli, Rovereto, Rossi, Amerano. In: De Pascale A,  
671 Del Lucchese A, Raggio O (eds) *La nascita della Paleontologia in Liguria: personaggi,*  
672 *scoperte e collezioni tra XIX e XX secolo*. Atti del Convegno (Finale Ligure Borgo, 22-23  
673 settembre 2006). Istituto Internazionale di Studi Liguri, Bordighera, pp 223–248
- 674 37. Bernabò Brea L (1946) *Gli Scavi nella Caverna delle Arene Candide. Parte I Gli Strati con*  
675 *Ceramiche*. Collezione di Monografie Preistoriche ed Archeologiche, I. Istituto di Studi  
676 Liguri, Bordighera



- 677 38. Bernabò Brea L (1956) *Gli Scavi nella Caverna delle Arene Candide (Finale Ligure)*. Parte  
678 Prima: *Gli Strati con Ceramiche: Campagne di Scavo 1948-50*. Collezione di Monografie  
679 Preistoriche ed Archeologiche, I. Istituto Internazionale di Studi Liguri, Bordighera
- 680 39. Sparacello VS, Panelli C, Rossi S, et al (2019) The re-discovery of Arma dell'Aquila (Finale  
681 Ligure, Italy): New insights on Neolithic funerary behavior from the sixth millennium BCE  
682 in the north-western Mediterranean. *Quat Int* 512:67–  
683 81doi.org/10.1016/j.quaint.2019.02.003.
- 684 40. Mannino MA, Talamo S, Goude G, et al (2018) Analisi isotopiche e datazioni sul collagene  
685 osseo degli inumati dell'Arma dell'Aquila. In: Biagi P, Starnini E, (eds) *Gli Scavi nell'Arma  
686 dell'Aquila (Finale Ligure, Savona): Le Ricerche e i Materiali degli Scavi del Novecento*.  
687 Quaderno 15. Società per la Preistoria e Protostoria della Regione Friuli-Venezia Giulia,  
688 Trieste, pp 183–188
- 689 41. Sparacello VS, Varalli A, Rossi S, et al (2019) Large-scale AMS dating on human skeletal  
690 series from Ligurian caves (northwestern Italy) and the Neolithic peopling of the  
691 northwestern Mediterranean. *Quat Int*doi.org/10.1016/j.quaint.2019.11.034.
- 692 42. Parenti R, Messeri P (1962) I resti scheletrici umani del Neolitico Ligure. *Palaeontographia  
693 Italica* 50:5–165
- 694 43. Marchi D, Sparacello VS, Shaw CN (2011) Mobility and lower limb robusticity of a  
695 pastoralist Neolithic population from North-Western Italy. In: Pinhasi R, Stock JY (eds)  
696 *Human bioarchaeology of the Transition to Agriculture*. John Wiley & Sons, New York, pp  
697 317–346
- 698 44. Villotte S, Knüsel CJ (2013) Understanding Enteseal Changes: Definition and Life Course  
699 Changes. *Int J Osteoarchaeol* 23:135-146
- 700 45. Villotte S, Assis S, Alves Cardoso F, et al (2016) In search of consensus: terminology for  
701 enteseal changes (EC). *Int J Paleopath* 13:49–55
- 702 46. Villotte S (2006) Connaissances médicales actuelles, cotation des enthésopathies: nouvelle  
703 méthode. *Bull Mem Soc Anthropol Paris* 18:65–85
- 704 47. Villotte S (2009) *Enthésopathies et activités des hommes préhistoriques. Recherche  
705 méthodologique et application aux fossiles européens du Paléolithique Supérieur et du  
706 Mésolithique*. Archaeopress, Oxford, 236 p

- 707 48. Villotte S, Castex D, Couallier V, et al (2010a) Enthesopathies as occupational stress  
708 markers: evidence from the upper limb. *Am J Phys Anthropol*, 142 (2):224–234
- 709 49. Dutour O (1986) Enthesopathies (lesions of muscular insertions) as indicators of the  
710 activities of Neolithic Saharan populations. *Am J Phys Anthropol* 71:221–224
- 711 50. Dutour O (2000) Chasse et activités physiques dans la Préhistoire: les marqueurs osseux  
712 d’activités chez l’homme fossile. *Anthropol Prehist* 111:156–165
- 713 51. Villotte S, Churchill SE, Dutour OJ, et al (2010b) Subsistence activities and the sexual  
714 division of labor in the European Upper Paleolithic and Mesolithic: evidence from upper  
715 limb enthesopathies. *J Hum Evol* 59:35–43
- 716 52. Villotte S, Knüsel CJ (2014) “I sing of arms and of a man. . .”: medial epicondylitis and the  
717 sexual division of labour in prehistoric Europe. *J Archaeol Sci* 43:168–174
- 718 53. Kennedy GE (1986) The relationship between auditory exostosis and cold water: a latitudinal  
719 analysis. *Am J Phys Anthropol* 71:401–415
- 720 54. Villotte S, Knüsel CJ (2016) External auditory exostoses and prehistoric aquatic resource  
721 procurement. *J Archaeol Sci: Rep* 6(4):633–6
- 722 55. Le Bras-Goude G, Binder D, Formicola V, et al (2006) Stratégies de subsistance et analyse  
723 culturelle de populations néolithiques de Ligurie: approche par l’étude isotopique ( $\delta^{13}\text{C}$  et  
724  $\delta^{15}\text{N}$ ) des restes osseux. *Bull Mem Soc Anthropol Paris* 18:45–55
- 725 56. Goude G, Binder D, Del Lucchese A (2014) Alimentation et modes de vie néolithiques en  
726 Ligurie. In: Bernabo Brea M, Maggi R, Manfredini A (eds) *Il Pieno Neolitico in Italia* (8-10  
727 juin Finale Ligure 2009). *Riv Studi Liguri* 77:371–387
- 728 57. Rowley-Conwy P (1997) The animal bones from Arene Candide (Holocene sequence): final  
729 report. In: Maggi R (ed) *Arene Candide: a functional and environmental assessment of the*  
730 *Holocene sequence (excavations Bernabò Brea-Cardini 1940–1950)*. *Istituto Italiano di*  
731 *paleontologia umana, Il calamo, Roma, ns 5, pp 153–277*
- 732 58. Molnar S (1972) Tooth wear and culture: a survey of tooth functions among some prehistoric  
733 population. *Curr Anthropol* 13:511–526
- 734 59. Brooks S, Suchey JM (1990) Skeletal age determination based on the os pubis: a comparison  
735 of the Acsádi-Nemeskéri and Suchey-Brooks methods. *Hum Evol* 5:227–238
- 736 60. Buckberry JL, Chamberlain AT (2002) Age estimation from the auricular surface of the  
737 ilium: a revised method. *Am J Phys Anthropol* 119:231–239

- 738 61. Schmitt A (2005) Une nouvelle méthode pour estimer l'âge au décès des adultes à partir de la  
739 surface sacro-pelvienne iliaque. *Bull Mem Soc Anthropol Paris* 17(1-2):1-15
- 740 62. Ubelaker DH (1989) *Human skeletal remains: excavation, analysis, interpretation,*  
741 *Taraxacum, Washington, 172 p*
- 742 63. Smith BH (1991) Standards of human tooth formation and dental age assessment. In:  
743 KelleyMA, Larsen CS (eds) *Advances in dental anthropology*. Wiley-Liss, New York, pp  
744 143-168
- 745 64. AlQahtani SJ, Hector MP, Liversidge HM (2010) The London atlas of human tooth and  
746 eruption. *Am J Phys Anthropol* 142:481-490
- 747 65. Schaefer M, Black S, Scheuer L (2009) *Juvenile osteology – a laboratory and field manual,*  
748 *Academic Press, New York, 384 p*
- 749 66. Ríos L, Cardoso HF (2009) Age estimation from stages of union of the vertebral epiphyses of  
750 the ribs. *Am J Phys Anthropol* 140:265-274
- 751 67. Cardoso HF, Ríos L (2011) Age estimation from stages of epiphyseal union in the presacral  
752 vertebrae. *Am J Phys Anthropol* 144:238-247
- 753 68. Boccone S, Micheletti Cremasco M, Bortoluzzi S, et al (2010) Age estimation in subadults  
754 Egyptian remains. *J Comp Hum Biol* 61:337-358
- 755 69. Buikstra JE, Ubelaker DH (1994) *Standards for Data Collection from Human Skeletal*  
756 *Remains, Arkansas Archaeological Survey Research Series No 44, Fayetteville, 218 p*
- 757 70. Loth SR, Henneberg M (1996) Mandibular ramus flexure: a new morphologic indicator of  
758 sexual dimorphism in the human skeleton. *Am J Phys Anthropol* 99:473-485
- 759 71. Bruzek J (2002) A method for visual determination of sex using the human hip bone. *Am J*  
760 *Phys Anthropol* 117:157-168
- 761 72. Thieme FP, Schull WJ (1957) Sex determination of the skeleton. *Hum Biol* 29:242-273.
- 762 73. Richman EA, Michel ME, Schuller-Ellis FP, et al (1979) Determination of sex by  
763 discriminant function analysis of postcranial skeletal measurements. *J Forensic Sci* 24:159-  
764 167.
- 765 74. Steyn M, İşcan MY (1997) Sex Determination from the Femur and Tibia in South African  
766 Whites. *Forensic Sci Int* 90(1-2):111-119
- 767 75. Murail P, Bruzek J, Braga J (1999) A new approach to sexual diagnosis in past populations,  
768 Practical adjustments from Van Vark's procedure. *Int J Osteoarchaeol* 9:39-53

- 769 76. Shaw C, Stock J (2009a) Intensity, repetitiveness, and directionality of habitual adolescent  
770 mobility patterns influence the tibial diaphysis morphology of athletes. *Am J Phys Anthropol*  
771 140:149–159
- 772 77. Shaw C, Stock J (2009b) Habitual throwing and swimming correspond with upper limb  
773 diaphyseal strength and shape in modern human athletes. *Am J Phys Anthropol* 140:160–172
- 774 78. Macintosh AA, Stock JT (2019) Intensive terrestrial or marine locomotor strategies are  
775 associated with inter- and intra-limb bone functional adaptation in living female athletes. *Am*  
776 *J Phys Anthropol* DOI: 10.1002/ajpa.23773
- 777 79. Sparacello VS, d’Ercole V, Coppa A (2015) A bioarchaeological approach to the  
778 reconstruction of changes in military organization among Iron Age Samnites (Vestini) from  
779 Abruzzo, central Italy. *Am J Phys Anthropol* 156:305–316
- 780 80. Ruff CB (2002) Long bone articular and diaphyseal structure in Old World monkeys and  
781 apes. I: locomotor effects. *Am J Phys Anthropol* 119:305–342
- 782 81. Nagurka ML, Hayes WC (1980) An interactive graphics package for calculating cross-  
783 sectional properties of complex shapes. *J Biomech* 13:59–64
- 784 82. Sparacello VS, Pearson OM (2010) The importance of accounting for the area of the  
785 medullary cavity in cross-sectional geometry: a test based on the femoral midshaft. *Am J*  
786 *Phys Anthropol* 143:612–624
- 787 83. Stock JT, Shaw CN (2007) Which measures of skeletal robusticity are robust? A comparison  
788 of external methods of quantifying diaphyseal strength to cross-sectional geometric  
789 properties. *Am J Phys Anthropol* 134:412–423
- 790 84. Macintosh AA, Davies TG, Ryan TM, et al (2013) Periosteal versus true cross-sectional  
791 geometry: a comparison along humeral, femoral, and tibial diaphysis. *Am J Phys*  
792 *Anthropol* 150:442–452
- 793 85. Ruff CB (2018) Quantifying skeletal robusticity. In: Ruff CB (ed) *Skeletal variation and*  
794 *adaptation in Europeans: Upper Paleolithic to the Twentieth Century*. John Wiley and Sons,  
795 Inc., New York, pp 39–47.
- 796 86. Ruff CB (2000) Body size, body shape, and long bone strength in modern humans. *J Hum*  
797 *Evol* 38:269–290
- 798 87. Trinkaus E, Ruff CB (2012) Femoral and tibial diaphyseal cross-sectional geometry in  
799 Pleistocene Homo. *PaleoAnthropology* 2012:13–62

- 800 88. Sparacello VS, Villotte S, Shackelford LL, et al (2017) Patterns of Humeral Asymmetry  
801 among Late Pleistocene Humans. *CR Palevol* 16(5–6):680–689
- 802 89. Trinkaus E, Churchill SE, Ruff CB (1994) Postcranial robusticity in Homo. II. humeral  
803 bilateral asymmetry and bone plasticity. *Am J Phys Anthropol* 93:1–34
- 804 90. Rhodes JA, Knüsel CJ (2005) Activity-related skeletal change in medieval humeri: cross-  
805 sectional and architectural alterations. *Am J Phys Anthropol* 128:536–546
- 806 91. Holt BM (2003) Mobility in Upper Paleolithic and Mesolithic Europe: evidence from the  
807 lower limb. *Am J Phys Anthropol* 122:200–215
- 808 92. Martiarena ML (2016) Analyse d'un marquer d'activité dans une population humaine  
809 préhistorique. M2 Thesis, Université libre de Bruxelles, Bruxelles
- 810 93. Polet C, Martiarena ML, Villotte S, et al (2019) Throwing activities among Neolithic  
811 populations from the Meuse River Basin (Belgium, 4500–2500 BC) with a focus on  
812 adolescents. *Child Past* 12(2):81–95
- 813 94. Crowe F, Sperduti A, O'Connell TC, et al (2010) Water-related occupations and diet in two  
814 Roman coastal communities (Italy, first to third century AD): correlation between stable  
815 carbon and nitrogen isotope values and auricular exostosis prevalence. *Am J Phys Anthropol*  
816 142:355–366
- 817 95. Standen VG, Arriaza BT, Santoro CM (1997) External auditory exostosis in prehistoric  
818 Chilean populations: A test of the cold water hypothesis. *Am J Phys Anthropol* 103:119–129
- 819 96. Velasco-Vazquez J, Betancor-Rodriguez A, Arnay-De-La Rosa M, et al (2000) Auricular  
820 exostoses in the prehistoric population of Gran Canaria, *Am J Phys Anthropol* 112:49–55
- 821 97. Villotte S, Stefanović S, Knüsel CJ (2014) External auditory exostoses and aquatic activities  
822 during the Mesolithic and the Neolithic in Europe: Results from a large prehistoric sample.  
823 *Anthropologie LII/1(1):73–89*
- 824 98. Cooper A, Tong R, Neil R, et al (2010) External auditory canal exostoses in white water  
825 kayakers. *Br J Sports Medicine* 44:144–147
- 826 99. Hurst W, Bailey M, Hurst B (2004) Prevalence of external auditory canal exostoses in  
827 Australian surfboard riders. *J Laryngol Otol* 118:348–351
- 828 100. Sparacello VS (2013) The Bioarchaeology of Changes in Social Stratification, Warfare,  
829 and Habitual Activities among Iron Age Samnites of Central Italy. PhD Thesis, University of  
830 New Mexico, Albuquerque

- 831 101. Villotte S, Samsel M, Sparacello VS (2017) The paleobiology of the two adult skeletons  
832 from Baouso da Torre (Bausu da Ture) (Liguria, Italy): implications for our understanding  
833 of Gravettian lifestyle. *Comptes Rendus Palevol* 16:462–473
- 834 102. Meyer C, Nicklisch N, Held P, et al (2011) Tracing patterns of activity in the human  
835 skeleton: An overview of methods, problems, and limits of interpretation. *J Comp Hum Biol*  
836 62:202–217
- 837 103. Jurmain R, Alves Cardoso F, Henderson C, et al (2012) Bioarchaeology's Holy Grail:  
838 The reconstruction of activity. In: Grauer AL (ed) *A Companion to Paleopathology*. Wiley-  
839 Blackell, New York, pp 531–552
- 840 104. Lazenby RA (1990) Continuing periosteal apposition II: the significance of peak bone  
841 mass, strain equilibrium, and age-related activity differentials for mechanical compensation  
842 in human tubular bones. *Am J Phys Anthropol* 82:473–484
- 843 105. Martin RB, Atkinson PJ (1977) Age and sex-related changes in the structure and strength  
844 of the human femoral shaft. *J Biomech* 10:223–231
- 845 106. Ruff C, Hayes W (1988) Sex differences in age-related remodeling of the femur and tibia.  
846 *J Orthop Res* 6:886–896
- 847 107. Agostini G, Holt BM, Relethford JH (2018) Bone functional adaptation does not erase  
848 neutral evolutionary information. *Am J Phys Anthropol* 166.10.1002/ajpa.23460.
- 849 108. Alves Cardoso FA, Henderson CY (2010) Enthesopathy formation in the humerus: Data  
850 from known age-at-death and known occupation skeletal collections. *Am J Phys Anthropol*  
851 141:550–560
- 852 109. Weiss E (2007) Muscle markers revisited: Activity pattern reconstruction with controls in  
853 a Central California Amerind population. *Am J Phys Anthropol* 133:931–940
- 854 110. Nikita E, Xanthopoulou P, Bertsatos A, et al (2019) A three-dimensional digital  
855 microscopic investigation of enthesal changes as skeletal activity markers. *Am J Phys*  
856 *Anthropol* DOI: 10.1002/ajpa.23850
- 857 111. Lieverse AR, Stock JT, Katzemberg MA, et al (2011) The bioarcheology of habitual  
858 activity and dietary change in the Siberian Middle Holocene. In: Pinhasi R, Stock J (eds)  
859 *Human bioarchaeology of the Transition to Agriculture*. Wiley-Liss, New York, pp 265–291.
- 860 112. Niinimäki S (2012) The relationship between musculoskeletal stress markers and  
861 biomechanical properties of the humeral diaphysis. *Am J Phys Anthropol* 147:618–628

- 862 113. Michopoulou E, Nikita E, Henderson CY (2017) A test of the effectiveness of the  
863 Coimbra method in capturing activity-induced enthesal changes. *Int J Osteoarchaeol*  
864 27:409–417
- 865 114. Michopoulou E, Nikita E, Valakos ED (2015) Evaluating the efficiency of different  
866 recording protocols for enthesal changes in regards to expressing activity patterns using  
867 archival data and cross-sectional geometric properties. *Am J Phys Anthropol* 158:557–568
- 868 115. Ibáñez-Gimeno P, Galtés I, Jordana X, et al (2013) Enthesal changes and functional  
869 implications of the humeral medial epicondyle. *IntJ Osteoarch* 23:211–220
- 870 116. Desse-Berset N, Desse J (1999) Les poissons. In: Tinè S (ed) *Il Neolitico della caverna*  
871 *delle Arene Candide (scavi 1972-1977)*. Istituto Internazionale di Studi Liguri, Bordighera, pp  
872 36–50
- 873 117. Di Bartolomeo J, Paparella M, Meyerhoff W (1991) Cysts and tumors of the external ear.  
874 In: Shumrick D, Gluckman J, Meyerhoff W (eds) *Otolaryngology*. 3rd edition, 2:1243–1258.
- 875 118. Fowler EP, Osmun PM (1942) New bone growth due to cold water in the ears, *Arch*  
876 *Otolaryngol Head Neck Surg* 36:455–466
- 877 119. Kusaka S, Hyodo F, Yumoto T, et al (2010) Carbon and nitrogen stable isotope analysis  
878 on the diet of Jomon populations from two coastal regions of Japan. *J Archaeol Sci* 37:1968–  
879 1977
- 880
- 881
- 882

<b>Individual ID</b>	<b>Analysis</b>	<b>Age Class</b>	<b>Age Dental</b>	<b>Age Poster.</b>	<b>Sex</b>	<b>AMS date cal. 95.4%</b>	<b>Chrono-cultural attribution</b>
Acqua o Morto 251+254	CSG*, EAE	Adult	30-50	U	M	4797-4695	SMP
Acqua o Morto 252+253	CSG*, ECs	Adult	30-50	U	F	5301-5073	ICC
Arene Candide 6PE 3 Perrando	CSG, ECs	Adult	30-50	30-50	M	failed (prob. V mill. BCE) (5657-4620) <sup>1</sup>	SMP
Arene Candide 1 Tinè	CSG*, EAE	Late adol.	15-18	15-17	M	4704-4374	SMP
Arene Candide 2 Tinè	CSG, EAE, ECs	Adult	30-50	30-50	M	5209-5011	ICC
Arene Candide 6622.1FI + 6730.2FI	CSG*, EAE, ECs	Adult	U	U	F	5208-5000	ICC
Arene Candide 6730.1FI	CSG*, ECs	Young Adult	U	20-30	F	4688-4540	SMP
Arene Candide 7PE	CSG, EAE, ECs	Adult	30-50	30-50	M	4767-4586	SMP
Arene Candide 8PE	CSG, EAE, ECs	Adult	30-50	30-50	M	4708-4555	SMP
Arene Candide II BB	CSG*, ECs	Adult	U	U	F	failed (prob. V mill. BCE)	SMP
Arene Candide III BB	CSG, EAE, ECs	Adult	30-50	30-50	M	4800-4619	SMP
Arene Candide IV BB (+ 6726FI + 6730.7FI)	CSG, EAE, ECs	Young Adult	20-30	20-30	F	4766-4558	SMP
Arene Candide IX BB	CSG, EAE, ECs	Adult	30-50	30-50	F	4779-4611	SMP
Arene Candide VI BB	CSG, EAE, ECs	Adult	30-50	U	M	4581-4457	SMP
Arene Candide VII BB	CSG, EAE, ECs	Adult	30-50	30-50	F	4778-4603	SMP
Arma dell'Aquila 1 Richard	CSG, EAE, ECs	Adult	30-50	30-50	M	5361-5221	ICC
Arma dell'Aquila 1 Zambelli	CSG, EAE, ECs	Adult	30-50	U	F	4723-4551	SMP
Arma dell'Aquila 2 Richard	CSG, EAE, ECs	Adult	>50	U	M	5213-5010	ICC
Arma dell'Aquila 3 Richard	CSG*, ECs	Adult	30-50	U	M	5202-4962	ICC
Arma dell'Aquila 5 Richard	CSG, EAE	Adult	30-50	U	F	5208-4956	ICC
Arma dell'Aquila RS5	CSG*	Adult	U	U	U	5750-5645	ICC
Arma dell'Aquila RS9	CSG*	Adult	U	U	F	5206-4911	ICC
Bergeggi (IV) 3573 + 3573bis	EAE	Adult	U	30-50	F	failed (prob. V mill. BCE)	SMP
Bergeggi 1 Modigliani	EAE	Adolescent	13-19 (12-15?)	12-13	U	4527-4370	SMP
Bergeggi 2 Modigliani	CSG*, EAE, ECs	Young Adult	20-30	30-50	M	4680-4494	SMP
Bergeggi 3 Modigliani	CSG, ECs	Adult	U	U	F	4488-4364	SMP
Bergeggi 4 Modigliani + PE01177, 6893FI	CSG, ECs	Young Adult	U	17-19	M	4680-4494	SMP
Bergeggi 5 Modigliani	CSG, EAE	Adult	U	U	F	4539-4374	SMP
La Matta 01085	EAE	Young Adult	20-30	U	M?	n/a (prob. V mill. BCE)	SMP



La Matta 01086	EAE	Adolescent	11.5-12.5	U	U	n/a (prob. V mill. BCE)	SMP
Nasino 1	CSG*, EAE, ECs	Late adol.	13-19	16-20	M	4232-4000	Chassean
Pian del Ciliegio Adult	CSG, ECs	Young Adult	20-30	20-30	M	4690-4544	SMP
Pipistrelli 3_El Muerto N3	CSG*, ECs	Adult	>20	U	M	4723-4614	SMP
Pipistrelli 5 dep23.I.28 Cirillo	CSG*, ECs	Adult	U	U	M	5016-4844	SMP
Pipistrelli 6 dep 23.II.41 Angelina	CSG*, ECs	Adult	U	30-50	M	4995-4810	SMP
Pollera 1 Tiné	CSG, EAE, ECs	Young Adult	20-30	20-30	F	4712-4552	SMP
Pollera 10PE	CSG, ECs	Young Adult	U	20-30	M	4701-4550	SMP
Pollera 110a	CSG*, ECs	Adult	U	U	F	4690-4544 <sup>2</sup>	SMP
Pollera 110b	CSG*	Adult	U	U	F	4690-4544 <sup>2</sup>	SMP
Pollera 12PE	CSG, EAE, ECs	Adult	30-50	30-50	F	4794-4687	SMP
Pollera 13PE	CSG, EAE, ECs	Adult	30-50	30-50	M	4686-4527	SMP
Pollera 14PE	CSG, EAE, ECs	Adult	30-50	30-50	F	4786-4616	SMP
Pollera 1PE Issel-Morelli	EAE	Adolescent	10-12	<11	U	4786-4616	SMP
Pollera 22PE	CSG*, ECs	Adult	U	30-50	M	4786-4616	SMP
Pollera 30PE	CSG, EAE, ECs	Adult	30-50	30-50	M	4689-4543	SMP
Pollera 31PE	CSG*	Adult	U	30-50	M	4701-4548	SMP
Pollera 32PE	CSG, ECs	Adult	U	30-50	M	failed (prob. V mill. BCE)	SMP
Pollera 33PE	CSG, EAE, ECs	Adult	30-50	30-50	F	4711-4555	SMP
Pollera 34PE	EAE	Adolescent	13-19	11-16	U	4723-4558	SMP
Pollera 6246PE	CSG, EAE, ECs	Adult	30-50	30-50	F	4650-4462	SMP
Pollera 6673.6FI	CSG*	Adult	U	U	U	4879-4724	SMP
Pollera 6690bis.3FI	CSG*, ECs	Young Adult	U	20-30	F	4794-4687	SMP
Arene Candide 6621.1	Osteometrics only	Adolescent	13-19	12-16	F	4726-4557	SMP
Arene Candide 6634.1+6626.1+6730.2tris	Osteometrics only	Adult	U	U	F	4792-4688	SMP
Arene Candide I BB 6731.1FI + 6627.2FI	Osteometrics only	Adolescent	U	13-17	U	4690-4544	SMP
Arene Candide V BB	Osteometrics only	Adolescent	c. 15	14-16	U	4720-4557	SMP
Pipistrelli 4_dep23.III.73_76	Osteometrics only	Young Adult	20-30	20-30	F	5207-4909	ICC

885 Table 1 – Individuals from the Neolithic in Liguria included in this study, indicating the analyses  
886 performed for each. Asterisks indicate the individuals for which CSG data was collected for this study (cf.  
887 the last CSG sample [32]). A more detailed list of individuals examined for this study, including their  
888 uncalibrated date and the museum where they are preserved, is available as Supplementary Information  
889 (excel file “Supplementary Information Tables A”). See also [41].

890 CSG: cross-sectional geometry; EAE: external auditory exostoses; ECs: enthesal changes; U: sex  
891 undetermined; M: male; F: female; SMP: Square Mouthed Pottery; ICC; Impresso-Cardial Complex.

892 <sup>1</sup> date from previous studies with large error (see excel file “Supplementary Information\_raw data by  
893 analysis”). <sup>2</sup> Date belongs to PO 110c, individual found in close association with PO 110a-b.

894 Table 1 – Individus néolithiques de Ligurie inclus dans l’étude, avec pour chacun d’eux une indication  
895 des analyses effectuées. Une liste plus détaillée, incluant les données radiocarbone non-calibrées et les  
896 lieux de conservation, est disponible dans l’annexe Table A. Voir également [41].

897 U: sexe indéterminé; M: homme; F: femme; <sup>1</sup> date provenant d’études antérieures avec une large erreur  
898 (voir l’annexe “Supplementary Information\_raw data by analysis”). <sup>2</sup> Date associée à PO 110c, un  
899 individu trouvé en étroite relation avec PO 110a-b.

900

	LUP			SMP			IRON			SMP-LUP	SMP-IRON
Males	n	mean	SD	n	mean	SD	n	mean	SD	HSD <sup>1</sup>	HSD
Z <sub>p</sub> humerus R	13	52.03	7.13	15	54.41	9.71	124	58.82	10.29	NS	NS
Z <sub>p</sub> humerus L	13	42.28	10.53	16	48.96	7.65	122	50.80	8.72	NS	NS
HUMBA	14	58.61	28.03	15	18.95	9.11	200	24.67	14.97	p < 0.0001	NS
Z <sub>p</sub> femur	18	106.24	10.53	13	102.90	14.47	144	101.62	15.05	NS	NS
I <sub>x</sub> /I <sub>y</sub> femur	18	1.40	0.25	13	1.30	0.17	156	1.07	0.18	NS	p < 0.0001
Z <sub>p</sub> tibia	16	109.41	15.78	13	105.82	19.29	94	102.11	16.67	NS	NS
I <sub>max</sub> /I <sub>min</sub> tibia	16	2.85	0.64	13	2.63	0.30	97	2.36	0.47	NS	NS
Females	n	mean	SD	n	mean	SD	n	mean	SD	HSD	HSD
Z <sub>p</sub> humerus R	4	49.24	8.06	11	45.20	4.30	53	48.69	6.92	NS	NS
Z <sub>p</sub> humerus L	5	48.15	7.51	13	46.28	5.00	52	46.71	6.11	NS	NS
HUMBA	4	12.53	2.81	12	6.4	5.66	97	13.81	10.64	NS	p < 0.05
Z <sub>p</sub> femur	7	96.75	13.39	12	94.81	11.40	68	93.75	13.71	NS	NS
I <sub>x</sub> /I <sub>y</sub> femur	11	1.26	0.27	12	1.15	0.17	71	0.99	0.18	NS	p < 0.05
Z <sub>p</sub> tibia	5	101.17	8.45	13	97.31	15.75	39	86.04	13.73	NS	p < 0.05
I <sub>max</sub> /I <sub>min</sub> tibia	6	2.14	0.27	13	2.34	0.32	41	2.11	0.40	NS	NS
Sexual Dimorphism		<b>LUP</b>			<b>SMP</b>			<b>IRON</b>			
Z <sub>p</sub> humerus R		NS <sup>2</sup>			p < 0.01			p < 0.0001			
Z <sub>p</sub> humerus L		NS			NS			p < 0.01			
HUMBA		p < 0.01			p < 0.001			p < 0.0001			
Z <sub>p</sub> femur		p < 0.1			NS			p < 0.001			
I <sub>x</sub> /I <sub>y</sub> femur		NS			p < 0.05			p < 0.01			
Z <sub>p</sub> tibia		NS			NS			p < 0.0001			
I <sub>max</sub> /I <sub>min</sub> tibia		p < 0.05			p < 0.05			p < 0.01			

Table 2 – Main CSG properties of the Ligurian Neolithic sample (SMP: Square Mouthed Pottery), and of the comparative samples (LUP: European Late Upper Palaeolithic; IRON: Orientalizing-Archaic Samnites from Abruzzo, Italy), by sex. The raw CSG data per individual are given in Supplementary Information Tables A. R: right; L: left. <sup>1</sup> Tukey’s Honest Significant Difference, post-hoc test of ANOVA among groups (LUP-SMP-IRON) by sex. <sup>2</sup> T-test between sexes, by period. NS: non-significant.

Table 2 – Principales propriétés géométriques les collections squelettiques néolithiques de Ligurie (SMP: culture des Vases à Bouche carrée) et des échantillons de comparaisons (LUP : fin du Paléolithique supérieur européen ; IRON : Age du Fer des Abruzzes, Italie centrale) suivant le sexe. Les données brutes par individu sont disponibles dans l’annexe Table A. R : droite ; L : gauche. <sup>1</sup> test des étendues de Tukey, Analyse de variance post-hoc (LUP-SMP-IRON) par sexe. <sup>2</sup> T-test suivant le sexe, par période. NS: non significatif.

	<b>LE Left</b>			<b>Fisher Exact test M vs F (A vs B+C)</b>
	<b>A</b>	<b>B</b>	<b>C</b>	
<b>Males</b>	6 (8)	3 (4)	2 (3)	NS
<b>Females</b>	5	2	1	
	<b>LE Right</b>			<b>Fisher Exact test M vs F (A vs B+C)</b>
	<b>A</b>	<b>B</b>	<b>C</b>	
<b>Males</b>	4	4 (5)	1	NS
<b>Females</b>	4 (5)	3	2	
	<b>Fisher Exact test R vs L (A vs B+C)</b>			
<b>Males</b>	NS			
<b>Females</b>	NS			
	<b>LE Asymmetry</b>			<b>Fisher Exact test (R+L vs NO)</b>
	<b>L</b>	<b>R</b>	<b>NO</b>	
<b>Males</b>	0	0	6	NS
<b>Females</b>	0	1	6	

Table 3 – Number of individuals showing enthesal changes (ECs) in the lateral epicondyle (common extensor origin) of the humerus in the Ligurian Neolithic sample, by sex. Numbers and p-values outside of parentheses refer to the SMP sample, numbers and p-values inside the parentheses refer to the pooled Neolithic sample. LE: lateral epicondyle. Scores: A, no change; B, minor changes; C, major changes. L: left; R: right; NO: no asymmetry; M: males; F: females.

Table 3 – Nombre d'individus présentant un changement enthésique (ECs) au niveau de l'épicondyle latéral (origine commune des extenseurs) de l'humérus dans l'échantillon néolithique de Ligurie, suivant le sexe. Les nombres et valeurs p. à l'extérieur des parenthèses font référence à l'échantillon SMP, celles entre parenthèses font référence à l'échantillon total. LE: épicondyle latéral. Scores: A, pas de changement; B, changements mineurs; C, changements majeurs. L: gauche; R: droit; NO: pas d'asymétrie; M: hommes; F: femmes.

	<b>CFT Left</b>			<b>Fisher Exact test M vs F (A vs B+C)</b>
	<b>A</b>	<b>B</b>	<b>C</b>	
<b>Males</b>	7 (9)	3	0	NS
<b>Females</b>	6 (7)	2	0	
	<b>CFT Right</b>			<b>Fisher Exact test M vs F (A vs B+C)</b>
	<b>A</b>	<b>B</b>	<b>C</b>	
<b>Males</b>	4	6	0	NS
<b>Females</b>	5 (6)	4	0	
	<b>Fisher Exact test R vs L (A vs B+C)</b>			
<b>Males</b>	NS			
<b>Females</b>	NS			
	<b>CFT ASYMM</b>			<b>Fisher Exact test M vs F (R+L vs NO)</b>
	<b>L</b>	<b>R</b>	<b>NO</b>	
<b>Males</b>	0	4	2	p < 0.1 (p < 0.05)
<b>Females</b>	0	1	6 (7)	

Table 4 – Number of individuals showing entheseal changes (ECs) in the area of attachment of the common flexor tendon (CFT; medial epicondyle of the humerus) in the Ligurian Neolithic sample, by sex. Numbers and p-values not in parentheses refer to the SMP sample, numbers and p-values in parentheses refer to the pooled Neolithic sample. Scores: A, no change; B, minor changes; C, major changes. L: left; R: right; NO: no asymmetry; M: males; F: females.

Table 4 – Nombre d'individus présentant un changement enthésique (ECs) au niveau de l'insertion commune des fléchisseurs de l'humérus (CFT) dans l'échantillon néolithique de Ligurie, suivant le sexe. Les nombres et valeurs p. à l'extérieur des parenthèses font référence à l'échantillon SMP, celles entre parenthèses font référence à l'échantillon total. Scores: A, pas de changement; B, changements mineurs ; C, changements majeurs. L: gauche; R: droit; NO: pas d'asymétrie; M: hommes; F: femmes.

	<b>UCL_Left</b>		<b>Fisher Exact test M vs F</b>	
	<b>A</b>	<b>P</b>		
<b>Males</b>	11 (16)	1	p = NS	
<b>Females</b>	11 (12)	1		
	<b>UCL_Right</b>		<b>Fisher Exact test M vs F</b>	
	<b>A</b>	<b>P</b>		
<b>Males</b>	3 (6)	7	p < 0.05 (p < 0.1)	
<b>Females</b>	10 (11)	2		
	<b>Fisher Exact test R vs L</b>			
<b>Males</b>	p < 0.01 (p < 0.01)			
<b>Females</b>	NS			
	<b>UCL ASYMM</b>			
	<b>L</b>	<b>R</b>	<b>NO</b>	<b>Fisher Exact test M vs F (R+L vs NO)</b>
<b>Males</b>	0	6	2 (5)	p < 0.01 (p < 0.05)
<b>Females</b>	0	1	10 (11)	

Table 5 – Number of individuals showing erosions/cavitations/geodes and/or fissures/well-defined pits (ECG+FP) in the anterior band of the ulnar collateral ligament in the Ligurian Neolithic sample, by sex. Numbers and p-values not in parentheses refer to the SMP sample, numbers and p-values in parentheses refer to the pooled Neolithic sample. A: no change; P: trait is present; L: left; R: right; M: males; F: females.

Table 5 – Nombre d'individus présentant une érosion/cavité/ géodes et/ou une fissure/dépression(ECG+FP) au niveau de l'insertion du fascia antérieur du ligament collatéral médial dans l'échantillon néolithique de Ligurie, suivant le sexe. Les nombres et valeurs p. à l'extérieur des parenthèses font référence à l'échantillon SMP, celles entre parenthèses font référence à l'échantillon total. Scores: A, pas de changement; P, changements present. L: gauche; R: droit; NO: pas d'asymétrie; M: hommes; F: femmes.

	<b>ME any change Left</b>		<b>Fisher Exact test M vs F</b>	
	<b>A</b>	<b>P</b>		
<b>Males</b>	7 (9)	3	NS	
<b>Females</b>	4 (5)	2		
	<b>ME any change Right</b>		<b>Fisher Exact test M vs F</b>	
	<b>A</b>	<b>P</b>		
<b>Males</b>	1 (2)	8	NS	
<b>Females</b>	3 (4)	6		
	<b>Fisher Exact test R vs L</b>			
<b>Males</b>	p < 0.05 (p < 0.05)			
<b>Females</b>	NS			
	<b>ME any change ASYMM</b>			
	<b>L</b>	<b>R</b>	<b>NO</b>	<b>Fisher Exact test M vs F (R+L vs NO)</b>
<b>Males</b>	0	5	1	NS
<b>Females</b>	0	2	4 (5)	

Table 6 – Number of individuals showing any entheseal change in the common flexor attachment site (scored B or C in Table 4) or in the anterior band of the ulnar collateral ligament (ECG or FP) in the Ligurian Neolithic sample, by sex. The table includes data exclusively from individuals for which both areas could be examined. Numbers and p-values not in parentheses refer to the SMP sample, numbers and p-values in parentheses refer to the pooled Neolithic sample. L: left; R: right; M: males; F: females.

Table 6 – Nombre d'individus présentant un changement enthésique au niveau de l'origine commune des flechisseurs (score B ou C dans le tableau 4) ou au niveau de l'insertion du fascia antérieur du ligament collatéral médial (ECG ou FP) dans l'échantillon néolithique de Ligurie, suivant le sexe. Le tableau inclus uniquement les individus pour lesquels les deux zones ont pu être examinées. Les nombres et valeurs p. à l'extérieur des parenthèses font référence à l'échantillon SMP, celles entre parenthèses font référence à l'échantillon total. L: gauche; R: droit; NO: pas d'asymétrie; M: hommes; F: femmes.



	<b>ME any change Left</b>		<b>Fisher Exact test M vs F</b>	
	<b>A</b>	<b>P</b>		
<b>Males</b>	9 (14)	3	NS	
<b>Females</b>	11 (12)	3		
	<b>ME any change Right</b>		<b>Fisher Exact test M vs F</b>	
	<b>A</b>	<b>P</b>		
<b>Males</b>	2 (5)	10	NS	
<b>Females</b>	6 (7)	6		
	<b>Fisher Exact test R vs L</b>			
<b>Males</b>	p < 0.05 (p < 0.05)			
<b>Females</b>	NS			
	<b>ME any change ASYMM</b>			
	<b>L</b>	<b>R</b>	<b>NO</b>	<b>Fisher Exact test M vs F (R+L vs NO)</b>
<b>Males</b>	0	7	1 (4)	p < 0.05 (p < 0.1)
<b>Females</b>	0	3	9 (10)	

Table 7 – Number of individuals showing any entheseal change in the common flexor attachment site (scored B or C in Table 4) or in the anterior band of the ulnar collateral ligament (ECG or FP) in the Ligurian Neolithic sample, by sex. The table include data from all individuals for which at least one area could be examined. Numbers and p-values not in parentheses refer to the SMP sample, numbers and p-values in parentheses refer to the pooled Neolithic sample. L: left; R: right; M: males; F: females.

Table 7 – Nombre d'individus présentant un changement enthésique au niveau de l'origine commune des flechisseurs (score B ou C dans le tableau 4) ou au niveau de l'insertion du fascia antérieur du ligament collatéral médial (ECG ou FP) dans l'échantillon néolithique de Ligurie, suivant le sexe. Le tableau inclus tous les individus pour lesquels au moins une zone a pu être examinée. Les nombres et valeurs p. à l'extérieur des parenthèses font référence à l'échantillon SMP, celles entre parenthèses font référence à l'échantillon total. L: gauche; R: droit; NO: pas d'asymétrie; M: hommes; F: femmes.

## Figures



Figure 1 – Geographical location of the Finalese area in Liguria (northwestern Italy), and location of the cave sites included in this study: 1) Arene Candide; 2) La Matta; 3) Pollera; 4) Arma dell’Aquila; 5) Pipistrelli; 6) Pian del Ciliegio; 7) Bergeggi; 8) Nasino.

Figure 1 – Localisations de la zone de Finale Ligure en Ligurie (Nord-Ouest de l’Italie) et des sites inclus dans cette étude : 1) Arene Candide; 2) La Matta; 3) Pollera; 4) Arma dell’Aquila; 5) Pipistrelli; 6) Pian del Ciliegio; 7) Bergeggi; 8) Nasino.

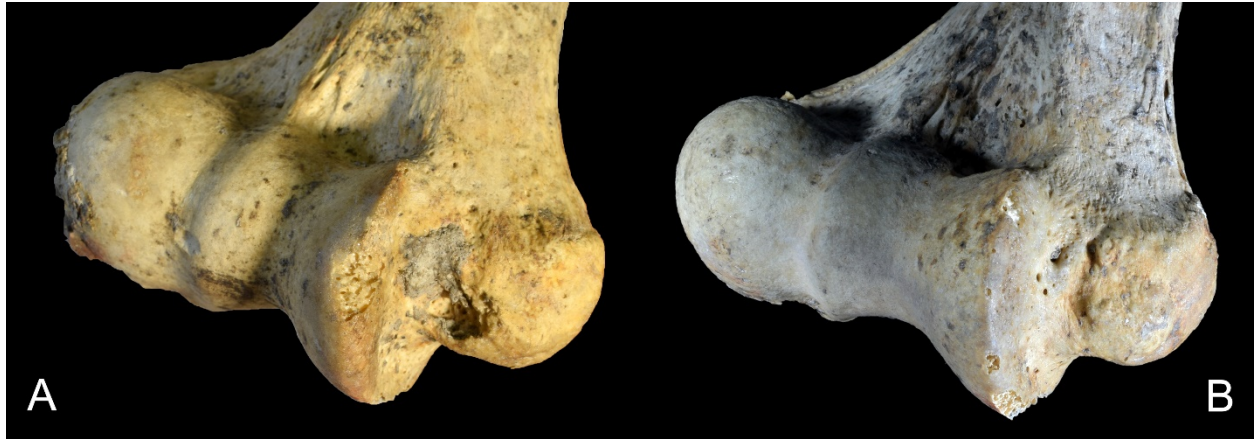


Figure 2 – Bony defects at the medial epicondyle, in the site of attachment of the anterior fascia of the ulnar collateral ligament. A) Individual Arene Candide 7 PE, despite the concretion obscuring part of the site, clearly shows a cavitation of the cortical surface and the formation of a geode, and was scored 1 for ECG. B) Individual Pollera 30, showing a fissure and well-defined pits in the area, but no interruption of the cortical surface. Scored 0 for ECG, 1 for ECG+FP.

Figure 2 – Défauts osseux au niveau de l'épicondyle médial, dans la zone d'insertion de la fascia antérieure du ligament collatéral médial. A) Individu Arene Candide 7 PE, qui en dépit de la concrétion qui recouvre la zone montre clairement un relief négatif au niveau de la surface et la formation d'une géode, avec un score 1 pour ECG. B) Individu Pollera 30, qui présente une fissure et des dépressions clairement visibles, mais sans rupture de la surface. Scoré 0 pour ECG, 1 pour ECG+FP.

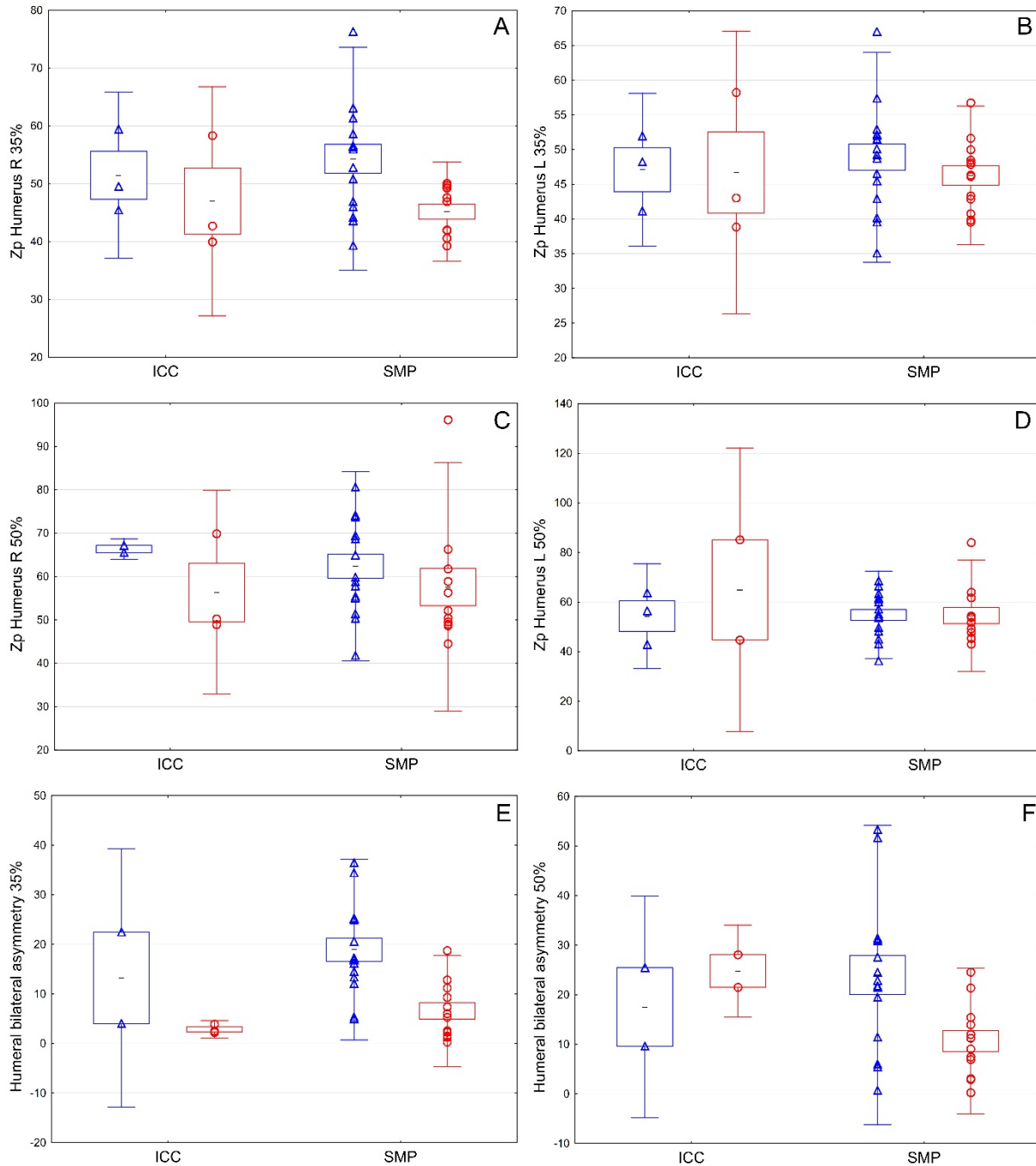


Figure 3 – Boxplots showing the main cross-sectional geometric (CSG) properties of the upper limb in the Ligurian Neolithic skeletal series, subdivided by chronological phase. The boxes indicate the standard error, the whiskers indicate two standard deviations from the mean. ICC: Impresso-Cardial Complex (c. 5800-5000 BCE); SMP: Square Mouthed Pottery (c. 5000-4300 BCE). F: females (circles); M: males (triangles); U: undetermined sex (squares). A) Mid-distal size-standardized right humeral robusticity; B) mid-distal size-standardized left humeral robusticity; C) midshaft size-standardized right humeral robusticity; D) midshaft size-

standardized left humeral robusticity; E) mid-distal humeral asymmetry in torsional rigidity (J) expressed as percentage; F) midshaft humeral asymmetry in torsional rigidity (J) expressed as percentage. All raw data are given in Supplementary Information Tables A.

Figure 3 – Boîtes à moustaches montrant les principales propriétés géométriques des sections transverses (CSG) du membre supérieur pour les collections squelettiques néolithiques de Ligurie, par phase chronologique. La boîte indique l'erreur standard et les moustaches montrent deux écart-types. ICC: complexe impresso-cardial (c. 5800-5000 BCE); SMP: culture des Vases à Bouche carrée (c. 5000-4300 BCE). F: femmes (cercles); M: hommes (triangles); U: sexes indéterminés (carrés). A) Robustesse humérale droite à mi distale de diaphyse, standardisée sur la taille; B) Robustesse humérale gauche à mi distale de diaphyse, standardisée sur la taille ;C) Robustesse humérale droite à mi diaphyse, standardisée sur la taille ; D) Robustesse humérale gauche à mi diaphyse, standardisée sur la taille ; E) Asymétrie humérale du moment polaire de l'aire (J) à mi distal de diaphyse exprimée en pourcentage ; F) Asymétrie humérale du moment polaire de l'aire (J) à mi diaphyse exprimée en pourcentage. Toutes les données brutes sont disponibles dans l'annexe Table A.

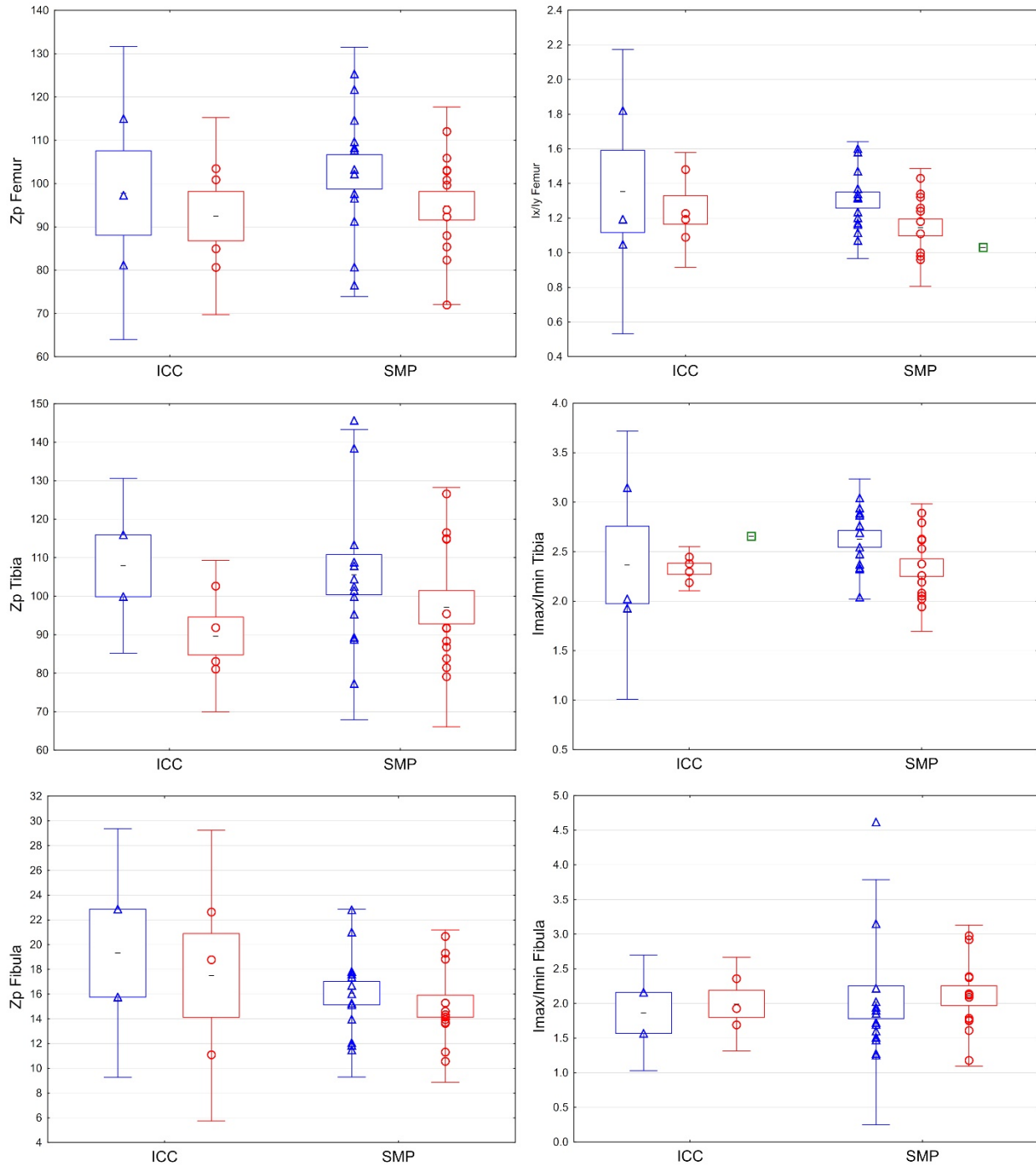


Figure 4 – Boxplots showing the main cross-sectional geometric (CSG) properties of the lower limb in the Ligurian Neolithic skeletal series, subdivided by chronological phase. The boxes indicate the standard error, the whiskers indicate two standard deviations from the mean. ICC: Impresso-Cardial Complex (c. 5800-5000 BCE); SMP: Square Mouthed Pottery (c. 5000-4300 BCE). F: females (circles); M: males (triangles); U: undetermined sex (squares). A) Midshaft size-standardized femoral robusticity; B) mid-distal femoral shape index  $I_x/I_y$ ; C) midshaft size-



standardized tibial robusticity; D) midshaft tibial shape index  $I_{\max}/I_{\min}$ ; E) midshaft size-standardized fibular robusticity; F) midshaft fibular shape index  $I_{\max}/I_{\min}$ . All raw data are given in Supplementary Information Tables A.

Figure 4 – Boîtes à moustaches montrant les principales propriétés géométriques des sections transverses (CSG) du membre inférieur pour les collections squelettiques néolithiques de Ligurie, par phase chronologique. La boîte indique l'erreur standard et les moustaches montrent deux écart-types. ICC: complexe impresso-cardial (c. 5800-5000 BCE); SMP: culture des Vases à Bouche carrée (c. 5000-4300 BCE). F: femmes (cercles); M: hommes (triangles); U: sexes indéterminés (carrés). A) Robustesse fémorale à mi diaphyse, standardisée sur la taille ; B) Indice de forme ( $I_x/I_y$ ) du fémur à mi distal de diaphyse ; C) Robustesse tibiale à mi diaphyse, standardisée sur la taille ; D) Indice de forme ( $I_{\max}/I_{\min}$ ) du tibia à mi diaphyse ; E) Robustesse fibulaire à mi diaphyse, standardisée sur la taille ; F) Indice de forme ( $I_{\max}/I_{\min}$ ) de la fibula à mi diaphyse. Toutes les données brutes sont disponibles dans l'annexe Table A.

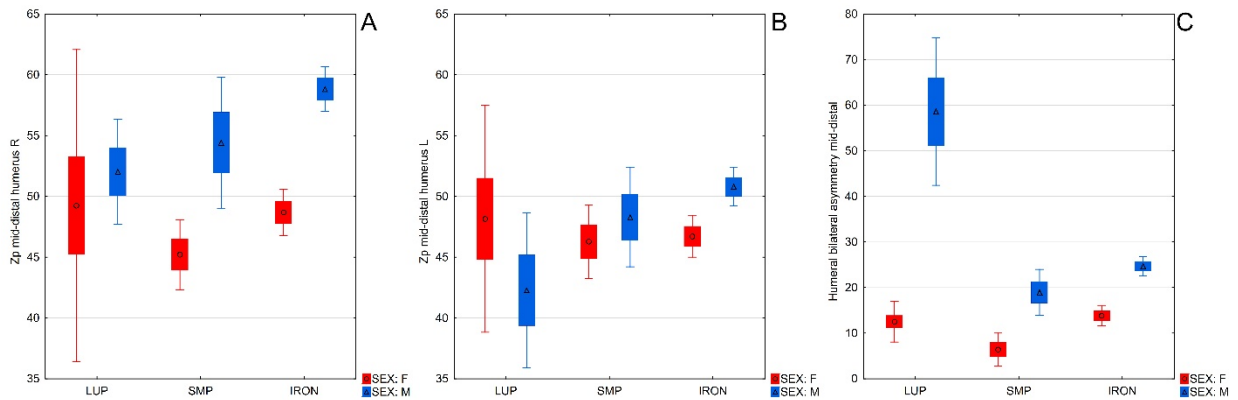


Figure 5 – Boxplots showing diachronic changes in humeral cross-sectional geometric (CSG) properties from the European Late Upper Palaeolithic (LUP), through the Square Mouthed Pottery Neolithic of Liguria (SMP), to the Orientalizing-Archaic Iron Age of Abruzzo, central Italy (IRON), by sex. The boxes indicate the standard error, the whiskers indicate  $1.96 \times SE$ . A) Mid-distal size-standardized right humeral robusticity; B) mid-distal size-standardized left humeral robusticity; C) mid-distal humeral asymmetry in torsional rigidity.

Figure 5 – Boîtes à moustaches montrant les variations diachroniques des propriétés géométriques des sections transverses (CSG) de l'humérus suivant le sexe. LUP : fin Paléolithique supérieur européen ; SMP : culture des Vases à Bouche carrée ; IRON : Age du Fer des Abruzzes, Italie centrale. La boîte indique l'erreur standard et les moustaches montrent  $1,96 * l'$ erreur standard. A) Robustesse humérale droite à mi distale de diaphyse, standardisée sur la taille; B) Robustesse humérale gauche à mi distale de diaphyse, standardisée sur la taille ;C) Asymétrie humérale du moment polaire de l'aire (J) à mi distal de diaphyse.

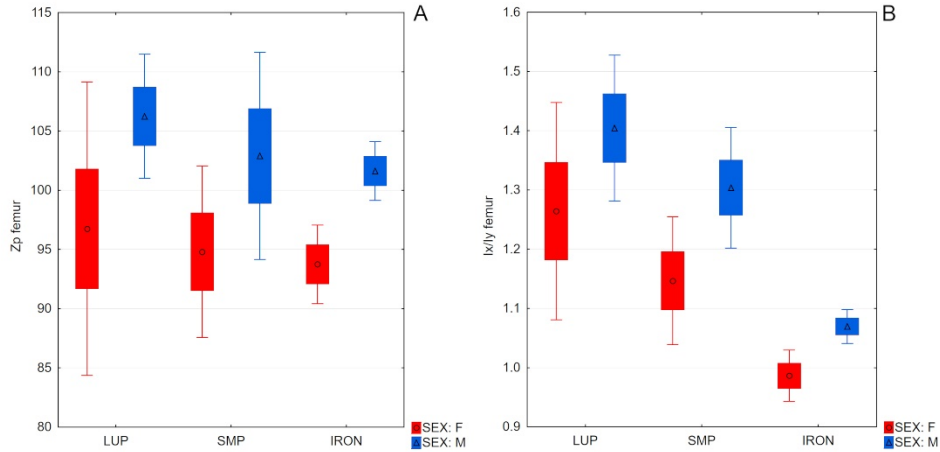


Figure 6 – Boxplots showing diachronic changes in femoral cross-sectional geometric (CSG) properties from the European Late Upper Palaeolithic (LUP), through the Square Mouthed Pottery Neolithic of Liguria (SMP), to the Orientalizing-Archaic Iron Age of Abruzzo, central Italy (IRON), by sex. The boxes indicate the standard error, the whiskers indicate  $1.96 \times SE$ . A) Midshaft size-standardized femoral robusticity; B) mid-distal femoral shape index  $I_x/I_y$ .

Figure 6 – Boîtes à moustaches montrant les variations diachroniques des propriétés géométriques des sections transverses (CSG) du fémur suivant le sexe. LUP : fin du Paléolithique supérieur européen ; SMP : culture des Vases à Bouche carrée ; IRON : Age du Fer des Abruzzes, Italie centrale. La boîte indique l'erreur standard et les moustaches montrent  $1,96 \times$  l'erreur standard. A) Robustesse fémorale à mi diaphyse, standardisée sur la taille ;B) Indice de forme ( $I_x/I_y$ ) du fémur à mi distal de diaphyse.

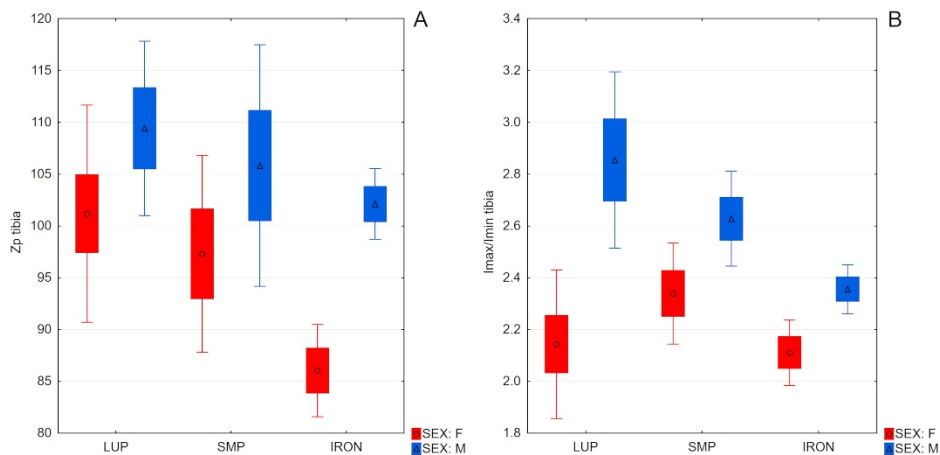


Figure 7 – Boxplots showing diachronic changes in tibial cross-sectional geometric (CSG) properties from the European Late Upper Palaeolithic (LUP), through the Square Mouthed Pottery Neolithic of Liguria (SMP), to the Orientalizing-Archaic Iron Age of Abruzzo, central Italy (IRON), by sex. The boxes indicate the standard error, the whiskers indicate  $1.96 \times SE$ . A) Midshaft size-standardized tibial robusticity; B) mid-distal tibial shape index  $I_{max}/I_{min}$ .



Italy (IRON), by sex. The boxes indicate the standard error, the whiskers indicate  $1.96 \times SE$ . A) Midshaft size-standardized tibial robusticity; B) midshaft tibial shape index  $I_{max}/I_{min}$ .

Figure 7 – Boîtes à moustaches montrant les variations diachroniques des propriétés géométriques des sections transverses(CSG) du tibia suivant le sexe. LUP : fin du Paléolithique supérieur européen ; SMP : culture des Vases à Bouche carrée ; IRON : Age du Fer des Abruzzes, Italie centrale. La boîte indique l'erreur standard et les moustaches montrent  $1,96 * l'$ erreur standard. A) Robustesse tibiale à mi diaphyse, standardisée sur la taille ;B) Indice de forme ( $I_{max}/I_{min}$ ) du tibia à mi de diaphyse.

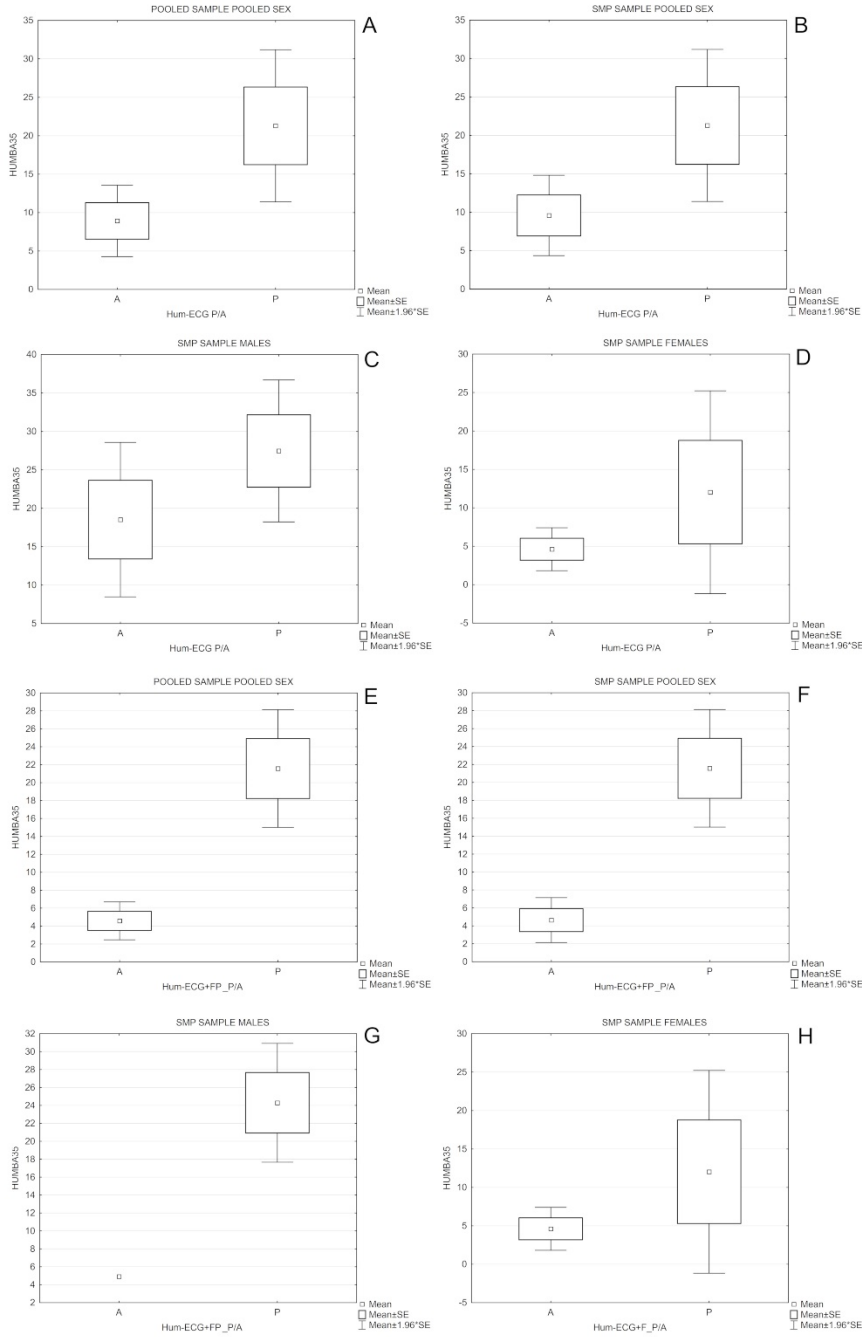


Figure 8 – Boxplots showing differences in mid-distal humeral bilateral asymmetry in torsional rigidity in subsamples based on the presence/absence of erosions/cavitations/geodes (ECG) or ECG plus fissures/well-defined pits at the medial epicondyle, in the site of attachment of the anterior fascia of the ulnar collateral ligament. The boxes indicate the standard error, the whiskers indicate  $1.96 \times SE$ . A) ECG presence/absence, pooled Ligurian Neolithic sample, pooled sexes; B) ECG presence/absence, SMP sample, pooled sexes; C) ECG presence/absence, SMP sample, males; D) ECG presence/absence, SMP sample, females; E) ECG+FP presence/absence, pooled Ligurian Neolithic sample, pooled sexes; F) ECG+FP

presence/absence, SMP sample, pooled sexes; G) ECG+FP presence/absence, SMP sample, males; H) ECG+FP presence/absence, SMP sample, females.

Figure 8 – Boîtes à moustaches montrant les différences d’asymétrie humérale du moment polaire de l’aire (J) à mi distal de diaphyse suivant la présence ou l’absence d’érosions/cavité/géodes (ECG) ou d’ECG associées à des fissures ou des dépressions au niveau de l’épicondyle médial, dans la zone d’insertion du fascia antérieur du ligament collatéral médial. La boîte indique l’erreur standard et les moustaches montrent  $1,96 * l'$ erreur standard. A) présence ou absence d’ECG, échantillons néolithiques et sexes confondus ; B) présence ou absence d’ECG pour l’échantillon SMP, sexes confondus ; C) présence ou absence d’ECG pour l’échantillon SMP, hommes ; D) présence ou absence d’ECG pour l’échantillon SMP, femmes ; E) présence ou absence d’ECG+FP, échantillons néolithiques et sexes confondus ; F) présence ou absence d’ECG+FP pour l’échantillon SMP, sexes confondus ; G) présence ou absence d’ECG+FP pour l’échantillon SMP, hommes ; H) présence ou absence d’ECG+FP pour l’échantillon SMP, femmes.

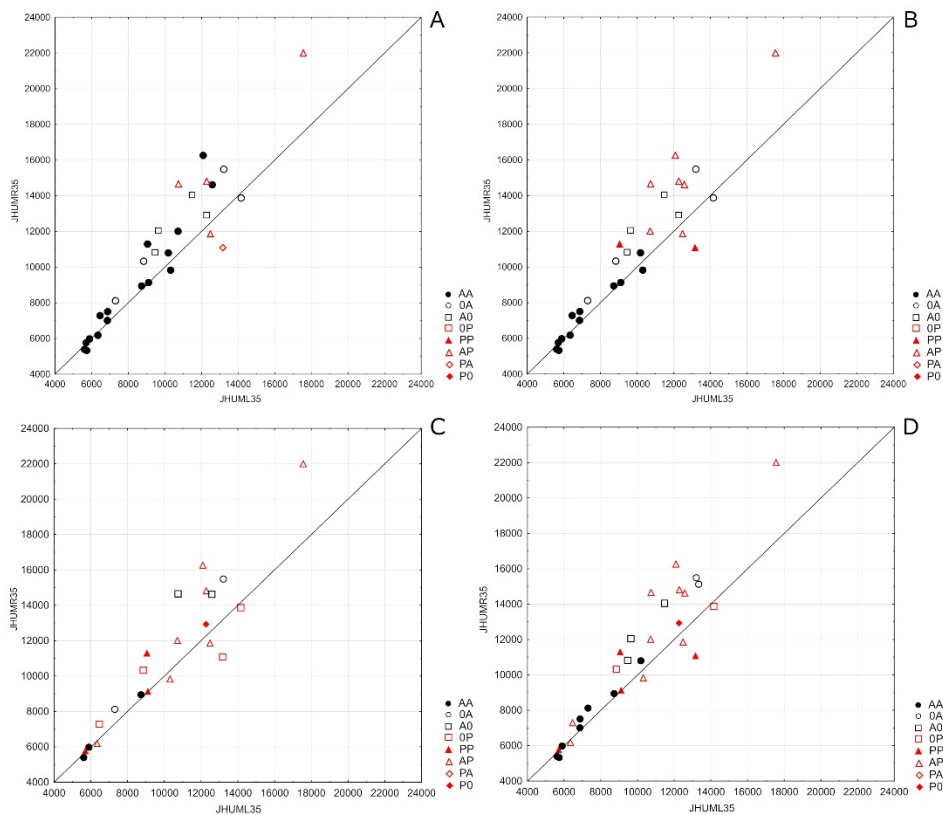


Figure 9 – Scatterplot of right humeral torsional rigidity (J) on left humeral torsional rigidity of the Ligurian Neolithic skeletal series, categorized on the basis of presence/absence and side of occurrence of A) ECG; B) ECG+FP; C) any change in the ME (UCL or CFT), considering only individuals for which both regions could be scored; D) any change in the ME (UCL or CFT),

considering also individuals for which only one region could be scored (see methods). The solid line indicates isometry. AA (black solid circles): left: trait absent, right: trait absent; OA (black circles) left: site not observable, right: trait absent; A0 (black squares) left: trait absent, right: site not observable; OP (red squares) left: not observable, right: trait present; PP (solid red triangles): left: trait present, right: trait present; AP (red triangles): left: trait absent, right: trait present; PA (red diamonds) left: trait present, right: trait absent; P0 (solid red diamonds) left: trait present, right: not observable.

Figure 9 – Diagramme bivarié du moment polaire de l'aire (J) à mi distal de diaphyse du côté gauche par rapport au côté droit pour les collections néolithiques, catégorisées sur la base de la présence ou de l'absence et de la latéralité de A) ECG ; B) ECG+FP ; C) tous les changements au niveau du ME (UCL ou CFT) en ne considérant seulement que les individus pour lesquels les deux zones peuvent être enregistrées ; D) tous les changements au niveau du ME (UCL ou CFT) en considérant tous les individus (voir la section méthode). La ligne indique l'isométrie. AA (cercles noirs pleins) : trait absent à gauche, trait absent à droite ; OA (cercles noirs) : trait non observable à gauche, absent à droite ; A0 (carrés noirs) : trait absent à gauche, non observable à droite ; OP (carrés rouges) : : trait non observable à gauche, présent à droite ; PP (triangles rouges pleins) : trait présent à gauche ; trait présent à droite ; AP (triangles rouges) : trait absent à gauche ; présent à droite ; PA (losanges rouges) : trait présent à gauche ; absent à droite ; P0 (losanges rouges pleins) : trait présent à gauche et non observable à droite.

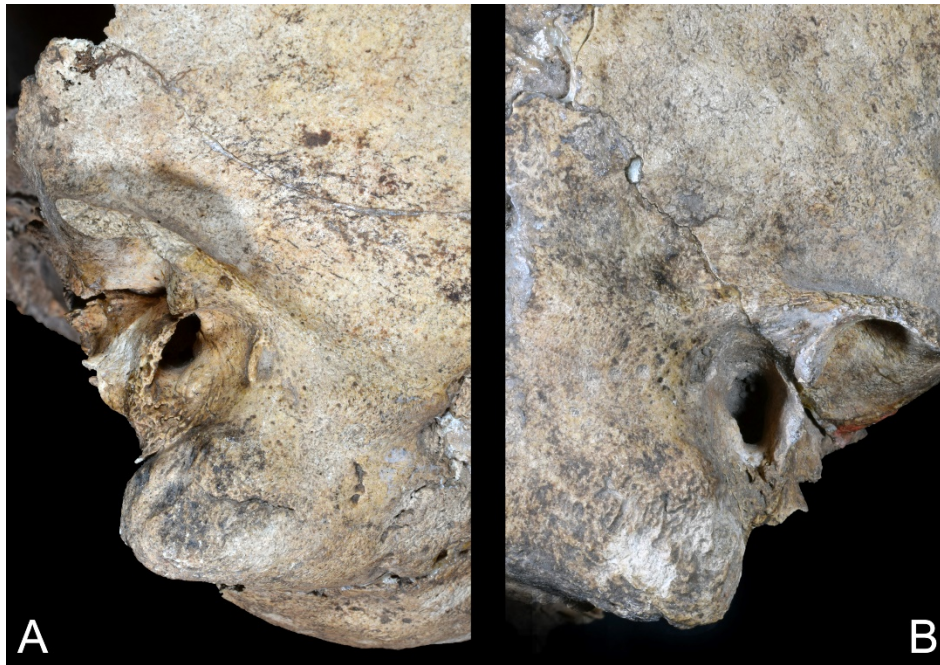


Figure 10 – Slight (score 1) bilateral external auditory canal exostosis (EAE) in the individual n°1 from Arma dell'Aquila, excavations Richard. A: left side; B: right side.

Figure 10. Exostose du canal auditif externe bilaterale légère (score 1) chez l'individu n°1 d'Arma dell' Aquila, fouilles Richard. A : côté gauche ; B : côté droit.